KILOHERTZ SESSION SUMMARY

Chairs: Georg Kirchner, Graham Appleby

Talks / presentations given:

- Hamal et al: Portable Pico Event Timer and SLR Control System
- Gibbs et al: Early Results of kHz SLR at Herstmonceux
- Degnan et al: LC Optical Gate for Monostatic kHz SLR System
- McGarry et al: SLR 2000: The Path Towards Completion
- Kirchner et al: Spin Parameters of AJISAI and GP-B from kHz SLR
- Kucharski et al: Lageos-1 Spin Determination from kHz SLR
- Kirchner et al: Measuring Atmospheric Seeing with kHz SLR

In addition: kHz SLR has a lot of unique advantages; just as an example, the graph below shows the significant improvement of the Peak-Minus-Mean value, when going from a standard 10-Hz system (old Graz SLR) to a kHz system; please note that such a statistical improvement is a necessary requirement if we want to think / talk about "mm-SLR" ☺

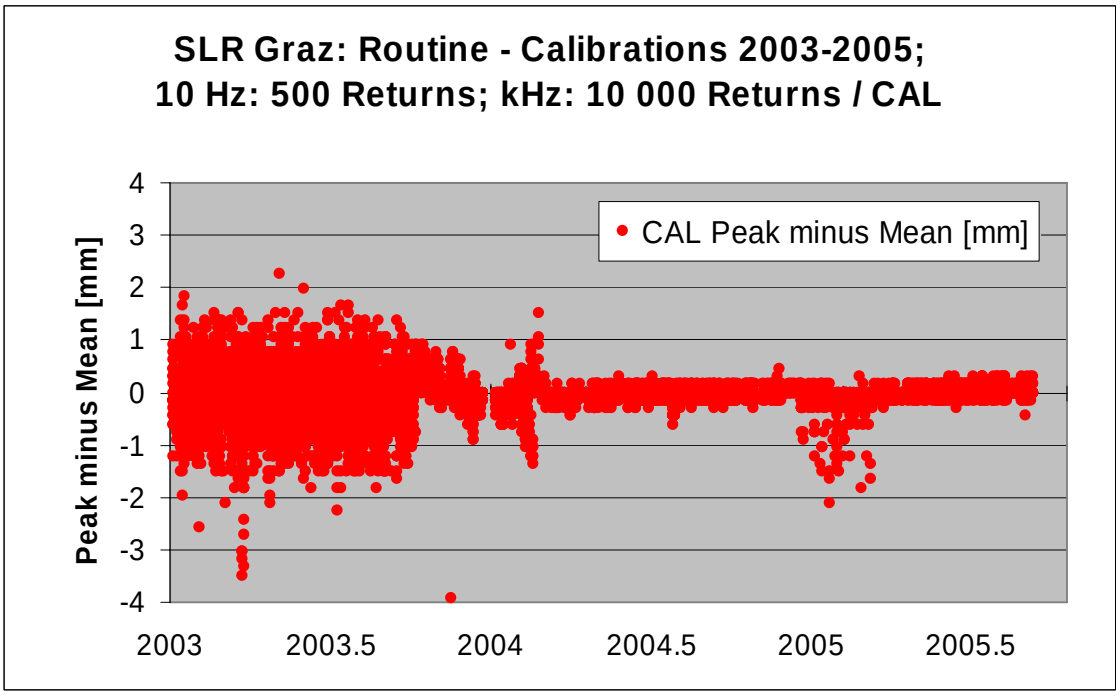

Portable Pico Event Timer and SLR Control (P-PET-C) System

Karel Hamal[1], Ivan Prochazka[1], Yang Fumin[2]

1. Czech Technical University in Prague, Brehova 7, 115 19 Prague 1, Czech Republic

2. Shanghai Observatory, Chinese Academy of Science, 80 Nandan Road, Shanghai, China

Contact: prochazk@troja.fjfi.cvut.cz

Abstract

We are reporting design, construction and parameters of the Portable Pico Event Timer and SLR Control (P-PET-C) System. It has been developed as a self-consistent system dedicated for the millimeter precision satellite laser ranging systems operating at high repetition rates up to 2 kHz. It provides real time control, measurement, data acquisition and data processing of the advanced satellite laser ranging station. It consists of the PET-C hardware and the software package. The system hardware has been developed on the basis of the Pico Event Timer (P-PET), which has been employed in laser ranging stations in Wettzell, Germany, TIGO Chile and in Portable Calibration Standard, a world wide accepted reference for pico-event timing for millimeter laser ranging. These systems have been operated at numerous stations around the world, including China, without any single failure for more than 8 years of continuous operation. The event timing is based on space qualified Dassault units no adjustment or re-calibration is needed. The 200MHz frequency generator was developed in FH Deggendorf. The real time control, measurement, data acquisition and data processing interface is based on the codes developed and operated at the satellite laser station in Graz, Austria, which is world first station operating a high repetition rate millimeter precision laser system. The real time control and data acquisition is provided by the built in PC. The first field operation was performed at the SLR Shanghai, China, 2006.

Goals

- Portable Pico Event Timer and SLRControl 2kHz
- Self-consistent portable unit
- Built in PC
- Dassault Timing Units
- Range Gate Generator
- T/R Pulse Overlap Avoidance
- Dedicated for Portable Calibration Standard 2k

Portable Pico Event Timer and SLR Control (P-PET-C) System

SLR Workshop

Freq module Deggendorf

2 kH SLR PC Card Graz

Pico Event Timer (P-PET)

Portable Pico Event Timer and SLR Control (P-PET-C) System

London 1998

Prague, Shanghai 2006

K.Hamal,I. Procházka, Yang Fumin, 15th ILRS Workshop,Canberra,2006

Portable Pico Event Timer and SLR Control (P-PET-C) System

P-PET-C Block Scheme

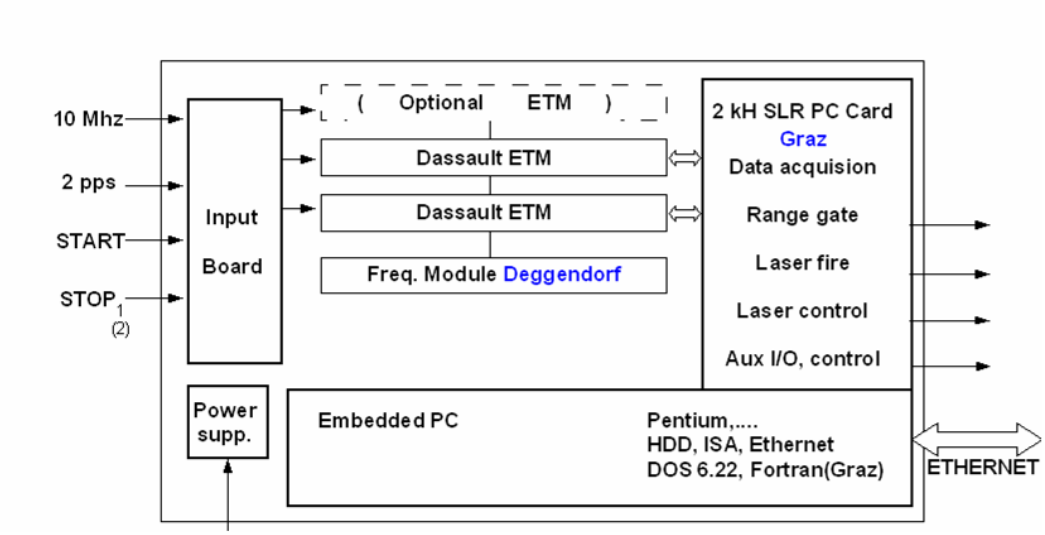

Portable Pico Event Timer and SLR Control (P-PET-C) System

Parametres

timing principle	event timing
timing resolution	1.2 ps
precision	3 ps
timing stability	better than 1 psec / K, / hour
maximum repetition rate	2 kHz
range gate	1 ns steps
	pulses “in space”
	maximum time un-limited
processes under control	epoch and range timing, range gate
	laser fire, laser control
	echo energy monitor interfacing
	T/R pulses collision avoidance
	additional epoch timing devices
	optional I/O
computer	built in, industrial PC
software package	Fortran :-) code, DOS 6.22
	field upgradable
dimension / mass / power	19‘ rack unit, 12‘ high / 30 kg / 200 W

K.Hamal,I. Procházka, Yang Fumin, 15th ILRS Workshop,Canberra,2006

Portable Pico Event Timer and SLR Control (P-PET-C) System

Portable Calibration Standard

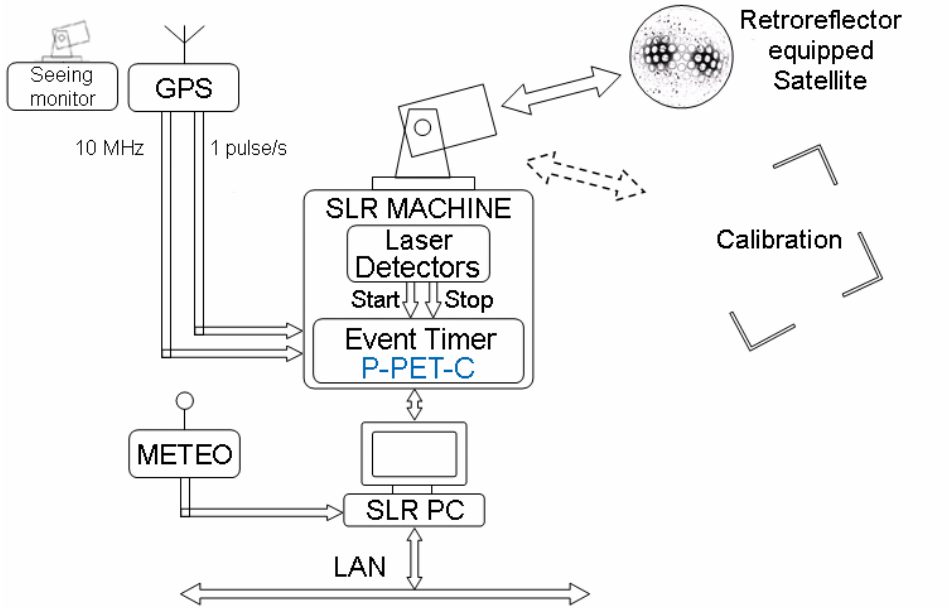

K.Hamal,I. Procházka, Yang Fumin, 15th ILRS Workshop,Canberra,2006

Portable Pico Event Timer and SLR Control (P-PET-C) System

Expected parametres: Equal Graz

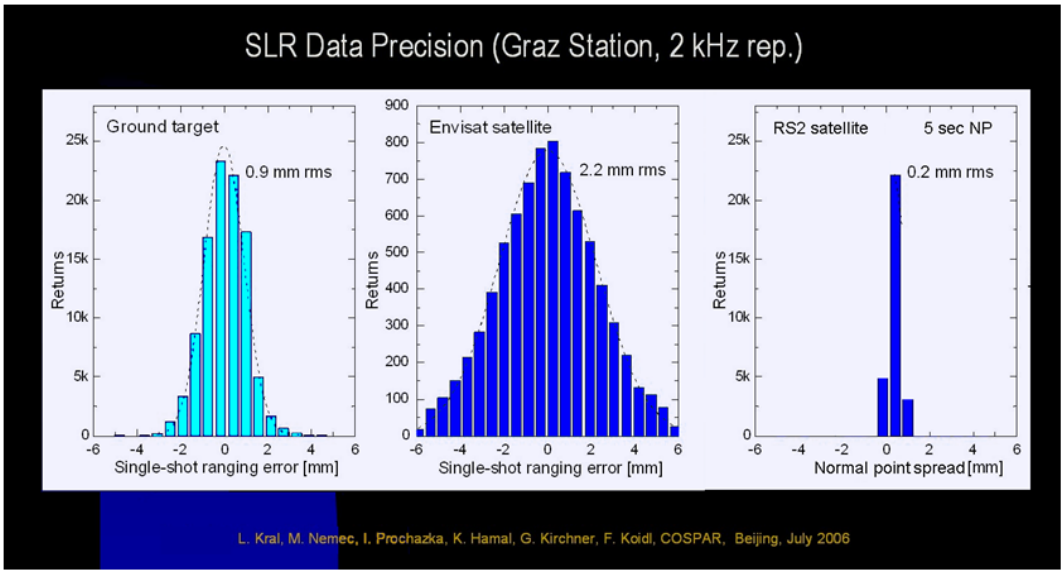

K.Hamal,I. Procházka, Yang Fumin, 15th ILRS Workshop,Canberra,2006

Portable Pico Event Timer and SLR Control (P-PET-C) System

Permanent installations of the PET timing technology

SLR station TIGO operated in Concepcion Chile,

PET4 operational since 1999.

WLRS , Satellite Laser Station Wettzell, Germany

PET4 operational since 1998

8 years no recalibration, no adjustment

K.Hamal,I. Procházka, Yang Fumin, 15th ILRS Workshop,Canberra,2006

Portable Pico Event Timer and SLR Control (P-PET-C) System

Conclusion

- 2kHz
- SLR control system
- Built-in PC
- Portable
- 8 years – no recalibration, no adjustment

- Ground RMS 1 MM Graz
- Satellite ERS2 RMS 2,8 MM Graz
- Normal Point RMS 0,2 MM Graz

- Price

K.Hamal,I. Procházka, Yang Fumin, 15th ILRS Workshop,Canberra,2006

Portable Pico Event Timer and SLR Control (P-PET-C) System

Shanghai indoor test, July 2006

Portable Pico Event Timer and SLR Control (P-PET-C) System

Shanghai outdoor test, July 2006

40W 2J

Some Early Results of Kilohertz Laser Ranging at Herstmonceux

Philip Gibbs, Christopher Potter, Robert Sherwood, Matthew Wilkinson,
David Benham, Victoria Smith and Graham Appleby

1. NERC Space Geodesy Facility, Herstmonceux Castle, Hailsham, UK, BN27 1RN.

Contact: pgib@nerc.ac.uk

Abstract

As part of its support of an upgrade and expansion of capability at the UK Space Geodesy Facility, the UK Natural Environment Research Council has provided funding to enable in-house development of kHz-rate laser ranging at the site. The scientific justification for this upgrade included the expectation of an increase in single shot precision furnished by the much shorter laser pulse-length, an increase in normal point precision from compression of a greater number of raw data points and much more rapid target acquisition via rapid searching.

The upgrade has proceeded in stages. Before we were able to consider kHz ranging we needed an event timing device able to record epochs of multiple events at kHz rates. To this end we built in-house the Herstmonceux Event Timer (HxET), which is based on three modules supplied by Thales. Following completion of HxET in August 2006, the device was thoroughly tested and found to agree with expectations in terms of linearity and precision. With HxET in place we were able to make our first tentative steps by late September into kHz calibration and satellite ranging. This paper presents some of our early problems and successes.

Basic Requirements for Kilohertz ranging

- A kHz laser.
- An event timer to record epochs of laser firing and detector triggering. This must be able to record epochs to an accuracy of a few picoseconds.
- A computer system(s) able to read ET, control the laser, display data and archive the data at kHz rates.
- Software to extract weak return signals from the higher noise levels generated by a C-SPAD running at kHz rates.
- Reduction software that can cope with the new features displayed in kHz data.

kHz Laser

Preparation for a kHz laser system began in 2003 with a visit to the SLR station in Graz, Austria. Graz had at that time recently purchased a kHz laser and was in the process of validating. This visit proved to be exceedingly useful in providing background knowledge necessary for the specification of a laser for the SGF. In 2004 final specifications for the kHz laser system were agreed and suppliers sought. The specification included a final output wavelength of 532nm with a pulse width of 10 – 15 ps at 1 – 2 kHz and a beam quality (M^2) better than 1.5. The ability of the laser to fire at ~10Hz to enable a smooth validation/transition from the old system to the 2 kHz system was also considered important. Other factors needed were the ability of the laser to fire on a shot by shot, variable rate basis under computer control, the ability of all the safety systems (lid locks, door interlocks and radar system) to be able to communicate with and inhibit firing, and the ability of the laser system to recover well after one of the frequent power cuts experienced at the SGF.

Given these specifications, a tender exercise identified two potential systems from High Q Lasers of Austria; one generating a power output of 0.4 mJ at 532nm and the second being capable of 1mJ at 532nm. With these power outputs the link budget calculations, to estimate return rates using a given laser system, were favourable. The following table shows our estimates for the link to the Lageos satellites in daytime, assuming an average amount of cirrus and a horizontal visibility of a poor 8km. The percentage value is the return rate of photons detected by the C-SPAD and the number in brackets is the resultant number of returns per 2-minute normal point:

Elevation	90°	50°	30°	25°
0.4mJ, 2kHz:	20% (12000);	8% (4000);	1% (500);	0.3% (150)
1.0mJ, 1kHz:	50% (15000);	19% (6000);	2% (700);	0.7% (150)

Following these calculations and financial considerations the 0.4mJ system was deemed sufficient but an extra long housing was ordered to enable possible future modification of the laser with an extra amplifier unit.

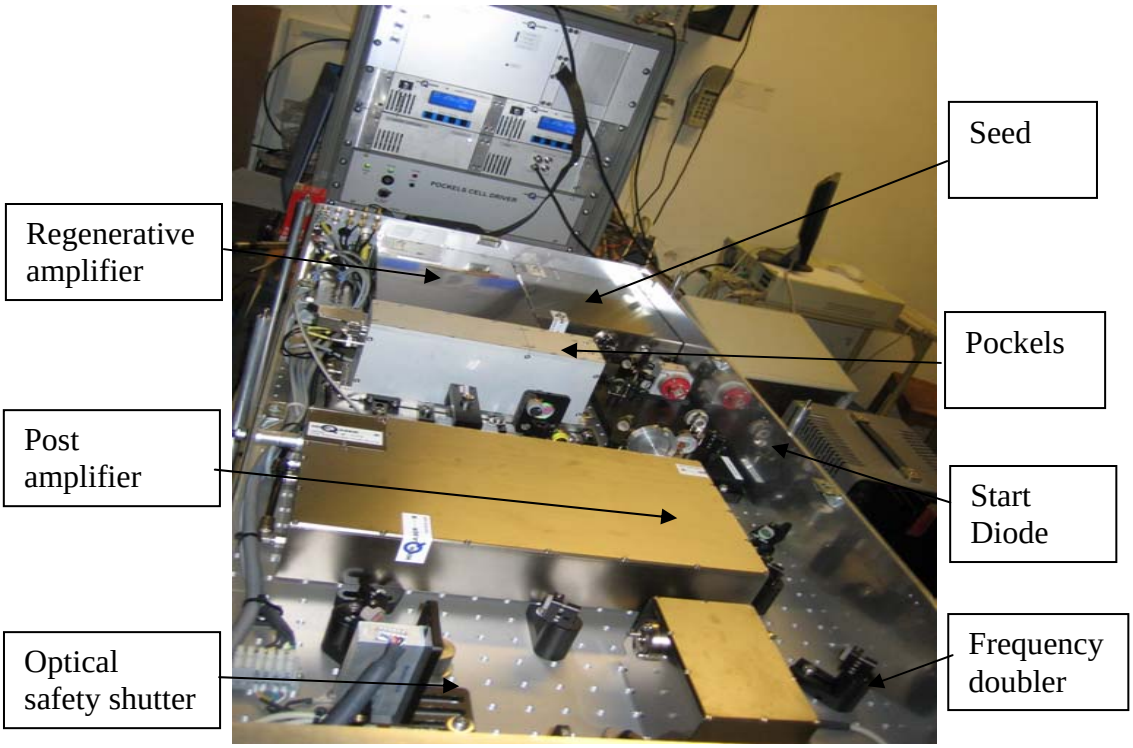

In summary, the specifications for the kHz laser are as follows:

- Nd: Vanadate picoREGEN laser from High-Q Lasers
- Pulse energy 0.5mJ at 532nm at 1kHz
  0.4mJ at 532nm at 2kHz
- Repetition rates of between 10 and 2000 (although large changes may require realignment). To date rates between 100 and 2000 Hz have been used without re-alignment.
- Pulse width is 10ps FWHM at 532nm.
- Upgradeable to >1mJ at 532.
- Firing predictability to 6ns.
- Typical lifetime of pump diode in excess of 10000 hours
- Beam quality – TEM_{00} M^2<1.5

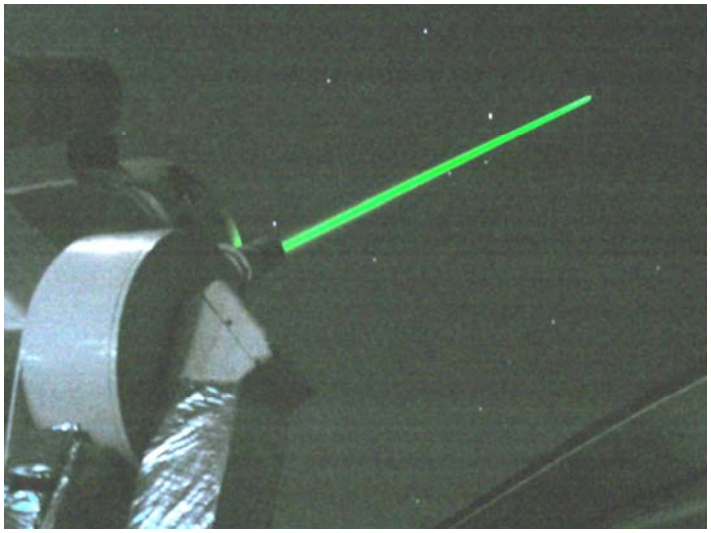

Shown here is a picture of the kHz laser at night

Event timer

A decision was made in 2004 to replace our SR620 timers with a timing system which would be linear across the range of times being measured and also be usable for a Kilohertz system. After investigating various options it was decided to build in-house an event timer with 3 Thales modules (1 clock module and 2 timing modules). The design of HxET included providing power supplies for each module plus some fifteen other power supplies, building an interface between the modules and the ranging computer, the ability to have start and stop signals as either NIM or TTL, and 1pps signal. It also had to include an onboard 1 kHz signal to monitor the difference between the two timing modules. The timer was completed in late July 2006 and ready for use soon after.

Initial tests of HxET using a split signal to the start and stop channels resulted in a total jitter of 7ps. If we assume an equal contribution from both the start and stop channels, this result gives a jitter of 5ps for each, in agreement with the specifications for the modules. Tests were also carried out using HxET to determine the behaviour of our SR620s across the whole timing range from local targets to the GNSS satellites; the results agreed with the results of previous identical tests carried out between PPET and the SR620s (Florence 1998). This we believe shows that there is agreement between PPET and HxET and that HxET is linear across the full range of current timing measurements. This calibration work is the subject of a further paper in these proceedings (Gibbs, Appleby and Potter, 2007).

Computer configuration.

The station computer configuration is as shown below. It comprises a Linux machine that is used to display and archive the data and run the reduction processes. This machine receives in real-time the data from the ranging PC (running under DOS) using TCPIP. The ranging PC communicates with HxET via a Programmable ISA card that was supplied to us by the GRAZ group. The ISA card also controls the Laser and arms the C-SPAD. The ranging PC also controls the telescope tracking, the safety radar, laser beam divergence and an iris in the receive optical path, as well as determining average return rate in real-time and maintaining a single photon return level via a neutral density wheel.

Real Time Display

Recognising that moving to kHz ranging will significantly reduce the signal to noise

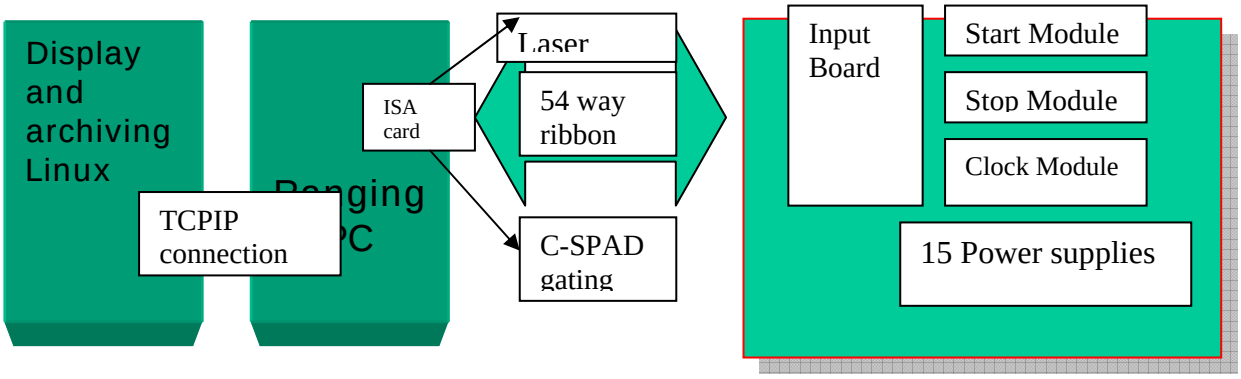

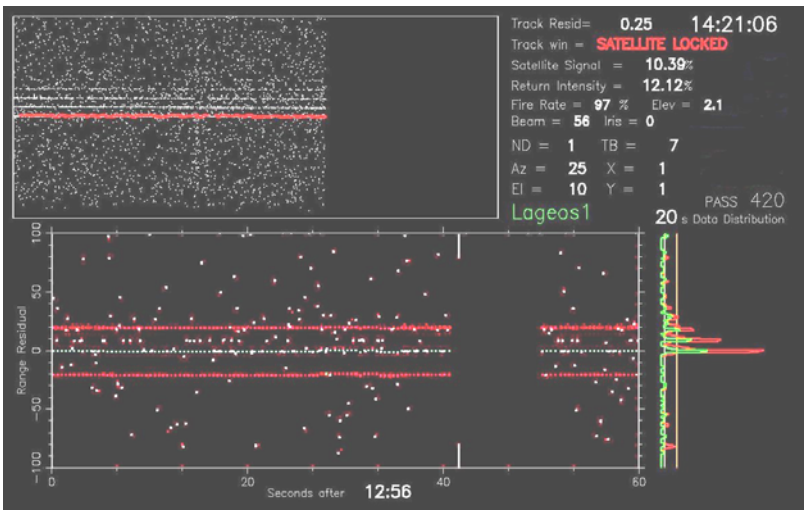

The display process runs on a Linux platform using a TCP-IP connection to the dedicated ranging PC. The display shows long term and short term range gate O-C values as well as a histogram of user defined time span to plot the intensity profile of the data.

ratio of the recorded data, early preparations were made to upgrade the display software. Previously, detection of track in the O-C real-time data within the range gate was aided by the known profile of the semi-train. The high rate data, lack of a semi-train and reduced satellite return signal associated with the low energy laser would make this procedure far more difficult, both for the observer and for the software.

The histogram technique is a very good indicator of the presence and the strength and stability of a satellite return signal and is used for automatic real-time track detection. The technique was developed and implemented for the 13Hz system with the eventual goal of preparing for kHz ranging. The 13Hz laser profile is an initial pulse followed by a significant semi-train, so to avoid tracking the wrong pulse within the semi-train a second histogram was designed in which later pulses are folded in to enhance the initial pulses. This technique exaggerates the first pulse and allows it to be continually tracked. The original (green) and altered (red) histogram profiles can be seen at the bottom right corner of the image above.

A confirmed satellite track is defined by a histogram bin reaching a level of 3-sigma above the background noise in the range gate. Two 3-sigma uncertainties for this track detection are calculated from the instantaneous histogram peaks and from peaks in short blocks of data over the histogram time period. If the satellite signal is strong and stable the software 'locks' onto the track. Once the satellite is locked, the track uncertainties are reduced to 2-sigma and only peaks falling within the newly-defined track window are considered as possible track.

The kHz laser has one dominant pulse and can be tracked with a single histogram. The high firing rate also means that a shorter histogram time span is sufficient, but additionally the histogram can pick out a weak intermittent track if it is given a longer

time span. From experimentation the software can lock on to a 1% satellite return signal with a 3 second time span and lock onto a 2% signal with a 2 second time span.

First Results

Testing of HxET and a full range of comparison tests between HxET and the SR620s were completed in late September 2006. Once completed, we designed the simplest possible software/hardware package that would enable us to obtain some high-rate satellite data as quickly as possible. To this end we simply used a pulse generator to fire the laser at approximately 2kHz. This simple system meant that we had no 'collision' control and as a result periods of high noise can be seen clearly in the data displayed below. We also did not attempt automatic control of return level (although manual control was still available) – in truth we were just happy to see that we were getting data. After just one week we had a software package that could collect data at kHz rates without any losses and then tried observing both in daylight and at night.

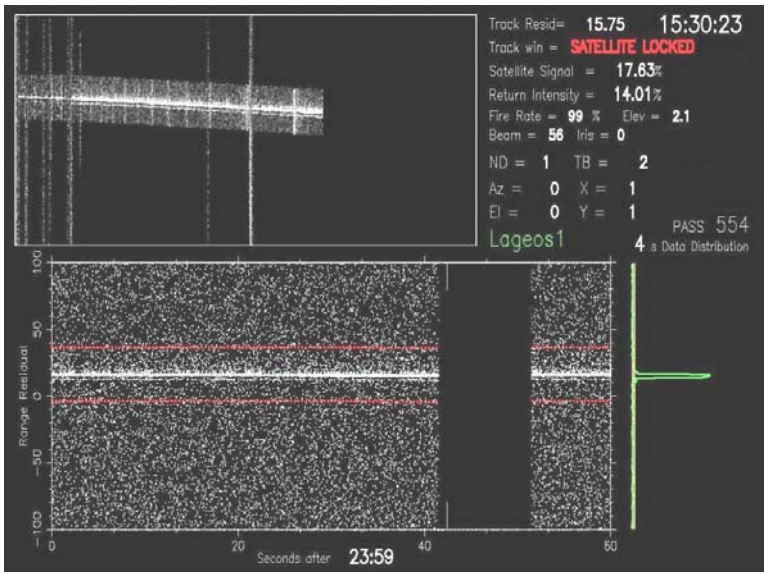

The long-term range gate displays the entire pass, as seen in the image at left. At high repetition rate this window becomes filled with noise points that mask any true track. However, by introducing a grayscale contrast for intensity of points, the track is revealed. This is a very powerful addition to the kHz tracking display, complementing the new histogram-based track determination.

During the daytime we were able to track successfully all satellites from Lageos' heights and lower except for Champ and Grace. At night we were able to range to all the ILRS satellites, again except Champ and Grace. These exceptions were caused by a software problem which has subsequently been solved.

One of the first things that was noticed was that many more noise events were detected than had been expected; initial tests indicated a noise increase of about a

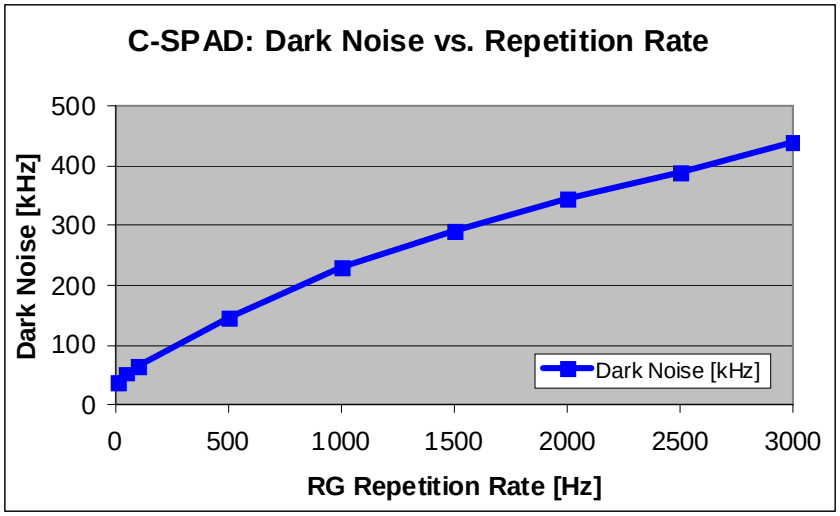

factor of 7 between tracking at 10Hz and at 2kHz. This appears to be due to an increase of dark noise in the C-SPAD as a function of arming rate. This effect had been discovered and quantified by the Graz group, and below is a plot provided by Graz of their results for C-SPAD noise vs. repetition rate.

To estimate the effect this increase of noise would have on our system we examined a histogram of noise collected at 2kHz.

Results from LAGEOS

Shown below is a plot of range O-C for Lageos-2 from October 4th 2006. Present is a number of interesting features. Clearly seen are the 'collision' periods when there are overlaps between incoming return pulses (C-SPAD gated on) and spurious detections of backscatter from outgoing laser light. Also apparent are pre-pulses and spurious other pulses because at the time of the observation the laser pockels cell was not optimally tuned. The uppermost O-C track represents the primary return signal.

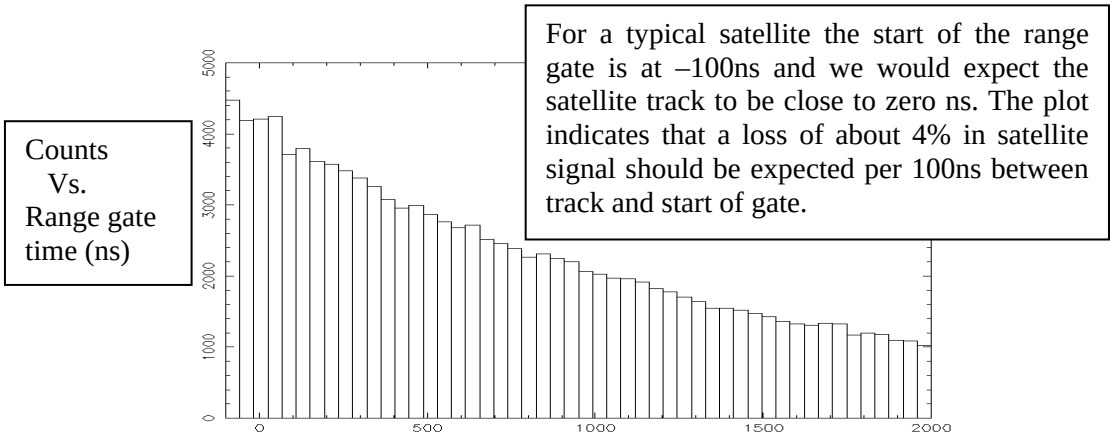

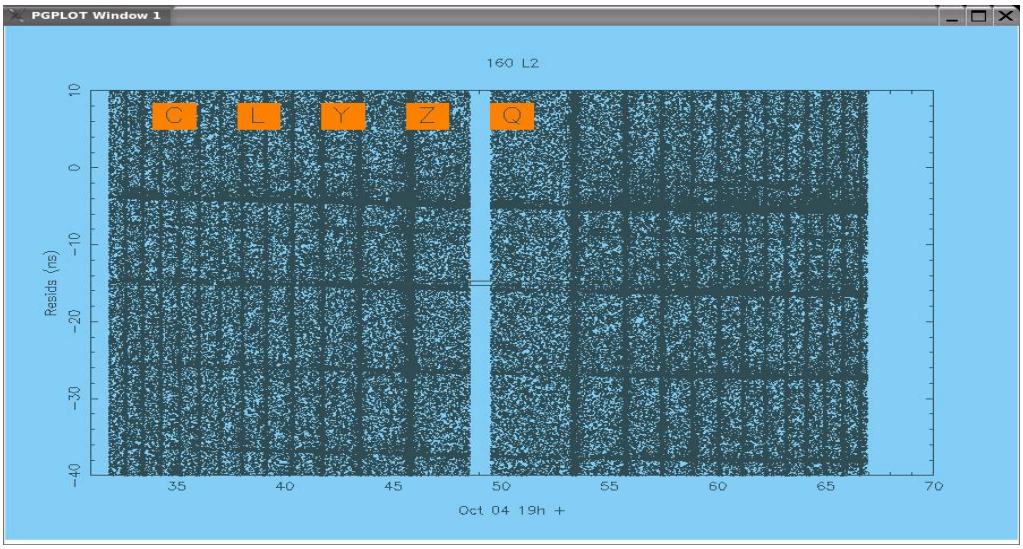

Having collected kHz data the next step was to use our current 10Hz reduction system to check whether there are any significant differences in the data, primarily in systematic effects that may compromise its quality.

The current reduction system comprises the following steps:

1. Extract a data set by a combination of linear and polynomial fitting to the raw O-C data. A minimum limit to the data set of ±0.75ns about the zero mean is imposed by the software to prevent the reduction being biased by the observer.

2. Fit an orbit to the extracted data, iteratively rejecting residuals at a 3-sigma level;
3. Remove this orbit from the entire raw data set and reject at 5-sigma level (yes 5);
4. Fit a smoothing function to this data set, rejecting at 2.5-sigma, using the routine DISTRIB that was produced and made widely available by A. Sinclair (SLRmail 0008).

Extraction of Data.

Below is a plot of the initial data set from which the observer will select the data to be passed to the orbital solution.

Gaussian Fit

Having selected the data as shown in the above plot an orbit is fitted to it. The orbit is then removed from the whole data set and residuals rejected at 5-sigma. We then need to know if this data set is different for the 10Hz and kHz systems

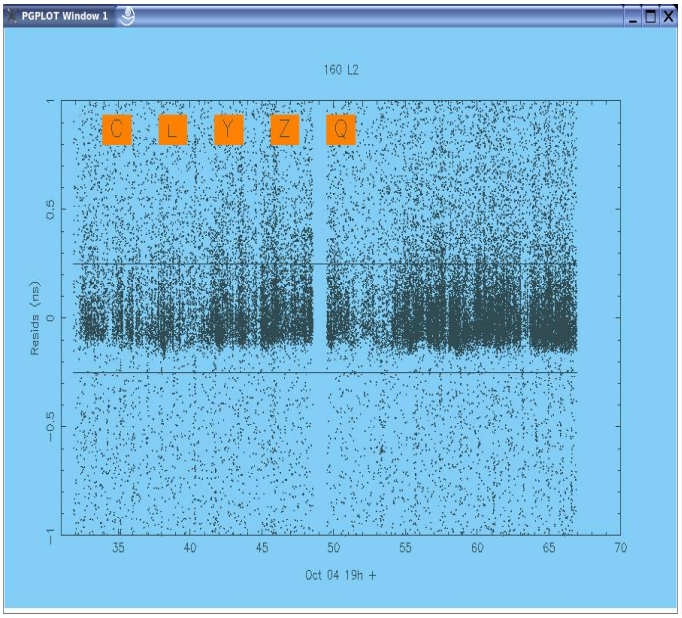

With the increase in background noise apparent at kHz rates it was felt that keeping at least ± 0.75ns of data would introduce too much noise in the preliminary signal extraction. We are currently experimenting with a reduced restriction of ± 0.25ns as shown in the plot, although the observer has the option of overriding these limits. In fact, better predictions, better software and higher-precision data means there is much less scatter in the residuals.

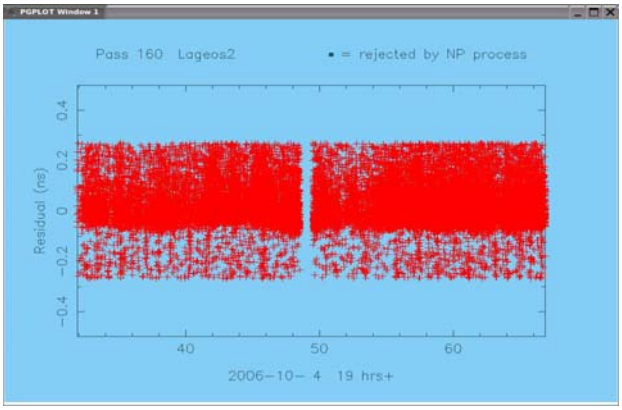

Pictured here is the data set after removing a best-fit orbit and rejecting residuals at a 5-sigma level. Apparent is a “significant” amount of noise below the track and some structure above the track. But is this behaviour significantly different to our current system?

At first glance it would appear that our reduction process is producing the same results for Lageos from both systems, but we have started a more detailed analysis in order both to define a robust reduction process and also to derive an accurate centre of mass correction. Previous work (Otsubo and Appleby, 2003) found that uniquely for the Herstmonceux single-photon system a Lageos centre of mass correction (CoM) of 245mm should be applied (cf 251mm for high-energy ILRS systems). It is important that once our new kHz data becomes available to the analysis community that we have also determined an accurate CoM correction, which may well be a few mm

different from the current 10Hz value. This ongoing work will be reported elsewhere, but the plot below shows the result of an initial investigation of the detailed post-reduction O-C distribution. The rapid rise of the leading edge is as expected and is a result of the short pulse length of the kHz laser, as suggested in the discussions above.

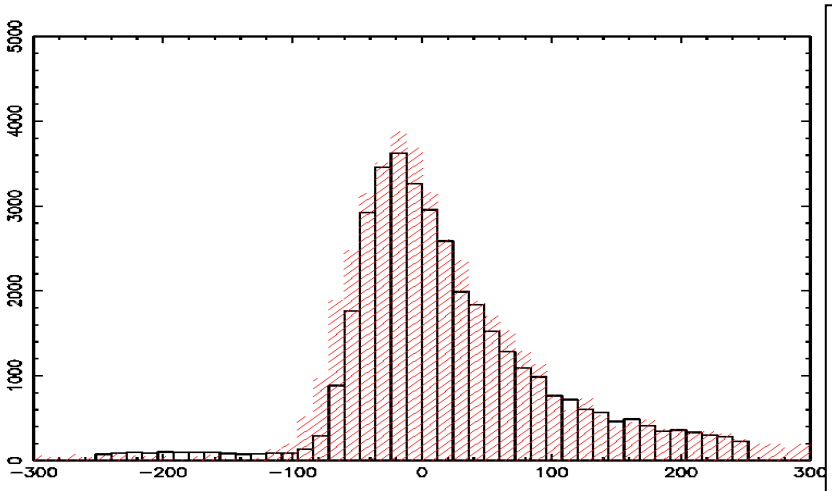

The distribution of the residuals from the two systems is very similar since the Lageos response dominates. As expected, the 10Hz data appears to be slightly broader as the timer and laser contributions are larger:

10Hz: 35ps for SR620
100ps for laser

KHz: 7ps for HxET
10ps for laser

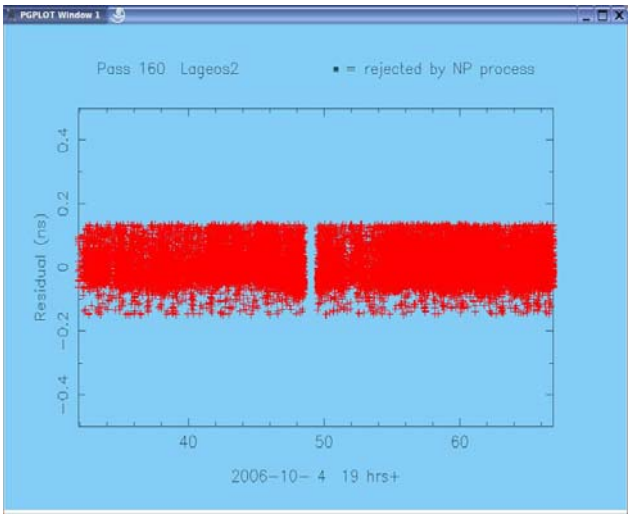

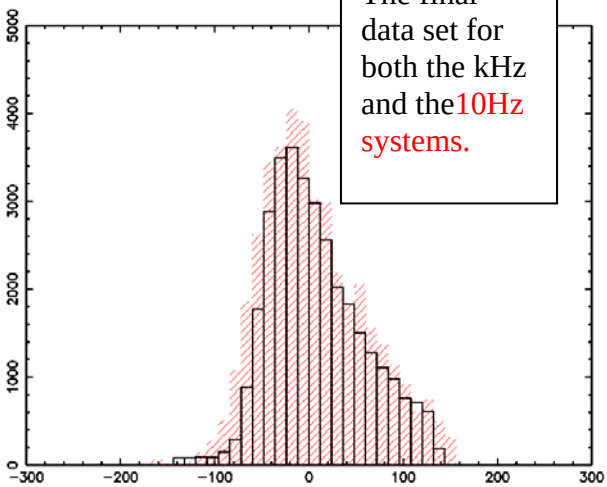

The final data set for both the kHz and the10Hz systems.

Shown above is the final data set for Lageos. There is clearly some noise below the track and the sharp cut off of dense data above may well have removed real observations.

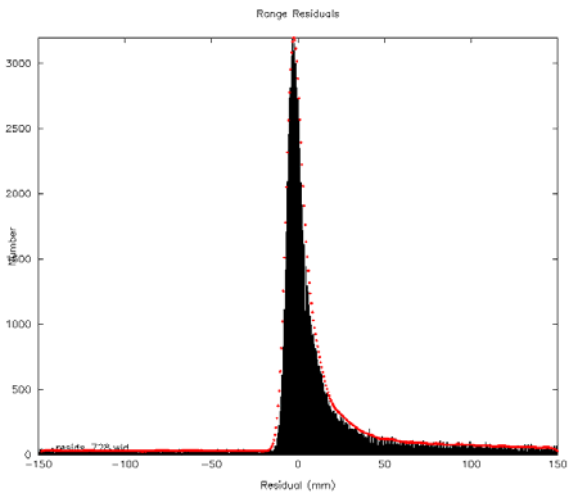

The smoothing function fitted to the distribution is shown in red, and will be used in an asymmetric filtering process to remove primarily leading-edge noise and in a model to determine an accurate CoM value.

Results from a small-array satellite (ENVISAT).

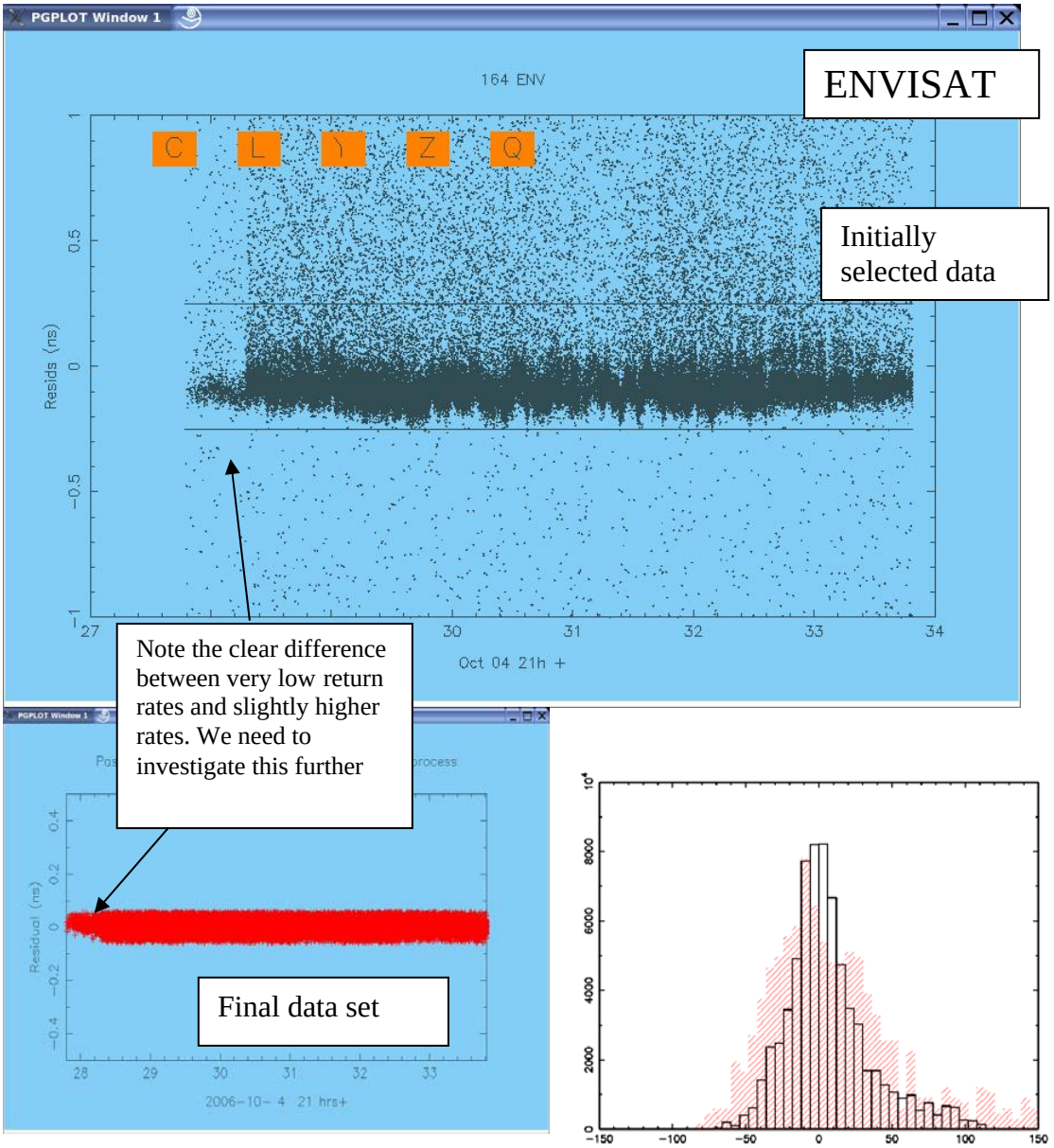

Conclusion

The SLR system at the UK Space Geodesy Facility is at an advanced stage of upgrade to kHz repetition rates, and incorporates a very accurate event timer. Paramount in the upgrade plans is that on-site reduction of the new data should not introduce any discontinuity into the long series of high quality laser data from the site.

Acknowledgement

We would like to thank the staff of the Institut for Space Research, Observatory Lustbuehel at Graz, Austria for their help and encouragement during the development of our kHz system at Herstmonceux.

References

[1] Gibbs, P., Appleby, G.M. and Potter, C.P., 2007. A re-assessment of laser ranging accuracy at SGF, Herstmonceux; *these proceedings*.

[2] Otsubo, T. and Appleby, G.M., 2003. System-dependent centre-of-mass correction for spherical geodetic satellites, JGR, vol. 108, doi:10.1029/2002JB002209.

Performance of a Liquid Crystal Optical Gate for Suppressing Laser Backscatter in Monostatic Kilohertz SLR Systems

John J. Degnan and Daniel Caplan

1. Sigma Space Corporation, 4801 Forbes Blvd., Lanham, MD 20706 USA.

Contact: John.Degnan@sigmaspace.com / Fax:+01-301-577-9466

Abstract

Some of the unique blocking features required by SLR2000 included a large aperture (15 mm), arbitrary polarization returns, a rapid 2 kHz cycle time, long and flexible blocking periods (up to 10% of each 500 microsecond interval between pulses), and adequate switching speeds to minimize data loss. After evaluating numerous potential approaches to optical gating, we determined that the use of a liquid crystal optical gate (LCOG) afforded the best overall protection. We have successfully implemented a 2 kHz LCOG which provides a 50 microsecond "blocked" interval, a 450 microsecond "unblocked" interval, a 10 microsecond rise and fall time on the blocking interval, approximately 90% transmission in "unblocked" mode, and a 659:1 reduction in backscattered radiation in "blocked" mode. Furthermore, the LCOG adapts readily to time shifting of the outgoing pulse.

Introduction

Since SLR2000 operates at a 2 kHz fire rate, multiple pulses are in the air at all times and, at various times within a given satellite pass, reflected signal photons arrive at the SLR2000 telescope at the same time a subsequent transmitted pulse is exiting the system. We refer to these events as "collisions". Since the range gate is open for some period surrounding the expected signal arrival time, the sensitive detector is exposed to backscattered laser radiation from both the instrument and the local atmosphere while in a high gain mode. In principle, backscatter from the atmosphere can be observed for up to 10% of the 500 microsecond laser fire interval. During this time, backscattered photons can cause significant charge transfer from the photocathode to the anode and, since the lifetime of a photocathode is dependent on the number of coulombs transferred, unsuppressed laser backscatter is a potentially life-limiting mechanism. In addition, since SLR2000 is designed to correct telescope pointing by balancing the photon returns in the four ranging detector quadrants, we believe that backscattered photons can interfere with the performance of the pointing correction algorithms by biasing the pointing error in the direction of the transmitter point ahead.

The quadrant segmented anode microchannel plate photomultiplier (MCP/PMT) in SLR2000 has recently been upgraded in order to achieve a factor of 3 to 5 improvement in detection efficiency and sensitivity. The bialkali photocathode tube built by Photek Inc. has been replaced by a significantly more expensive Hamamatsu tube with a less mature but higher efficiency (30% to 40%) GaAsP photocathode. In order to protect the tube from backscattered laser radiation and extend photocathode life, SLR2000 incorporates two design features. The first feature involves periodically changing the laser repetition rate to avoid "collisions" between outgoing pulses and incoming signal photons. This eliminates backscatter during the most critical period when the detector is gated "on", minimizes data loss, and helps to prevent corruption of the quadrant detector pointing correction. We have recently investigated the inclusion of an optical gate which acts as a second layer of defense by

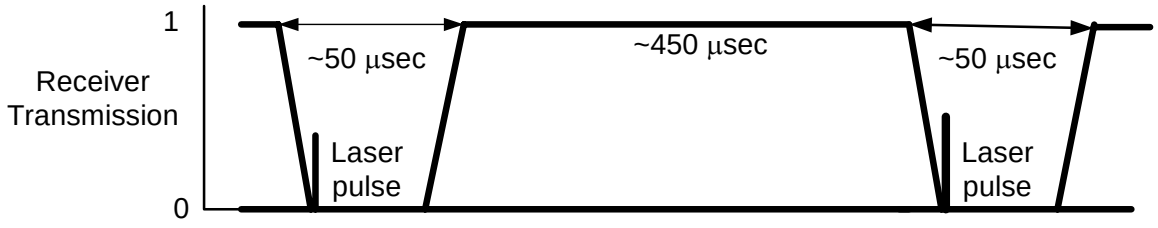

Figure 1. *Performance of the ideal optical gate for suppressing laser backscatter in SLR2000 operating at a 2 kHz rate.*

suppressing backscatter impinging on the photocathode even during less critical times when the detector is gated "off". The ideal performance of the "ideal optical gate" is illustrated in Figure 1. To minimize loss of signal while providing maximum protection, a successful optical gate in SLR2000 must possess the following characteristics:

- Operate at SLR2000 2 kHz laser fire rate,
- Accommodate the 13 mm receiver beam diameter on the optical bench,
- Block atmospheric backscatter for up to 50 microseconds following laser fire,
- Provide high backscatter extinction in blocked mode,
- Provide high signal transmission in unblocked mode,
- Provide a fast transition between blocked and unblocked modes,
- Accommodate variable fire rate used to avoid "pulse collisions",
- Can take advantage of linearly polarized light in two SLR2000 receiver channels if necessary.

We considered various approaches to optical gating including mechanical, electro-optical, acousto-optical, and liquid crystal and rated them with respect to transition speed, aperture, transmission, and ability to provide a long "open" mode. Liquid crystal gates were found to have the best overall performance with electro-optical being deemed less appropriate due to the need to maintain high voltages on the crystals for long periods of time. Our conclusions are summarized in Table 1.

Table 1. *Comparative performance of various optical gating approaches.*

Gating Approach	**Speed**	**Aperture**	**Transmission**	**Gate Duration**
Mechanical	Poor	Poor	Excellent	Poor
Electro-optic	Excellent	Good	Good	Poor (2-3 kV)
Acousto-optic	Good	Poor	Fair	Good
Liquid Crystal	Good	Good	Good	Good ($\pm$30V)

Experiment

The Liquid Crystal Optical Gate (LCOG) takes advantage of the fact that, in SLR2000, the received signal is split based on polarization. This is a consequence of our unique passive Transmit/Receive switch which permits the transmitter and receiver to share the entire telescope aperture simultaneously while experiencing low loss in either path [Degnan, 2004]. In a typical configuration, the LCOG normally acts as a time dependent polarization rotator placed between two crossed polarizers. The first polarizer defines the input polarization. Relatively low voltage (< ±30 VDC) waveforms applied to the crystal align the liquid crystals and rotate the propagating light in a time dependent manner. The action of the second polarizer on the rotated light creates the time varying transmission function of the gate.

As will be described later, the current SLR2000 receiver configuration uses uncrossed polarizers in each receiver leg although crossed polarizers could be employed with a relatively minor design change. For this reason, we conducted our laboratory tests with both crossed and uncrossed polarizer pairs. The signs of the waveform voltages were chosen accordingly to approximate the performance of the ideal gate depicted in Figure 1. Figure 2 provides a block diagram and photo of our test setup.

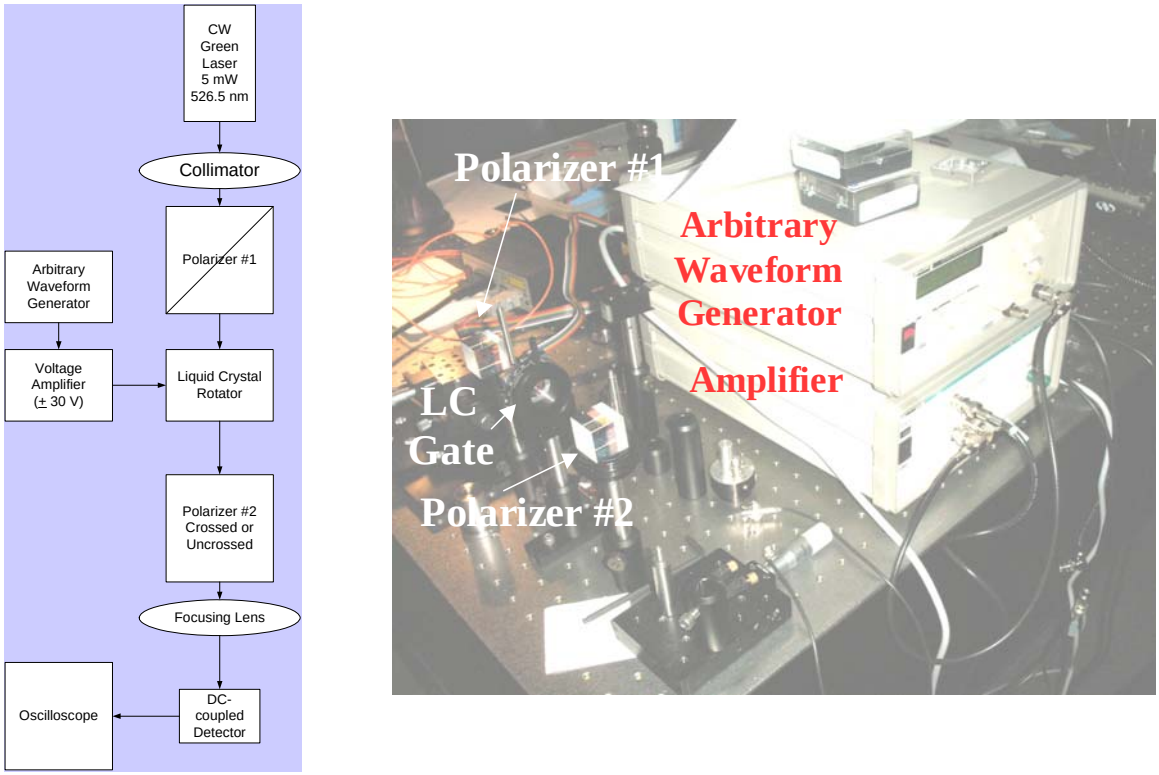

Figure 2: *Block diagram and photo of the laboratory test setup.*

The required waveform was programmed into a high bandwidth Arbitrary Waveform Generator (AWG) and iterated to best approximate the ideal transmission function. The low voltage output of the AWG was amplified to the required ± 30VDC by a separate amplifier module and applied to the flying leads of the Liquid Crystal Rotator manufactured by Boulder Nonlinear Systems, Inc. . Collimated light from a CW green laser was passed through the LCOG and focused onto a DC-coupled detector whose output was displayed on an oscilloscope. Prior to inserting the Liquid Crystal Rotator (LCR), the extinction of the crossed CVI cube polarizers was measured to be 6222:1 in reasonable agreement with the specified value of 10,000:1 and demonstrated the

sensitivity of our measurement approach. A summary of the peak optical gate transmissions and extinctions obtained with different polarizer combinations is given in Table 2. Not surprisingly, the best extinction of 659:1 during "closed" periods was obtained with the normal crossed polarizer configuration whereas the P/P and S/S configurations, corresponding to the current SLR2000 receiver configurations (see Figure 4), provided significantly poorer extinctions of 164:1 and 82:1 respectively. The transmission of the gate during "open" periods was comparable in all cases, varying over a narrow range between 89.3% and 92.1%.

Table 2. *Summary of experimental transmissions and extinctions for various configurations of crossed and uncrossed polarizers.*

Polarizer 1	Liquid Crystal Gate	Polarizer 2	Transmission (gate open)	Extinction (gate closed)
P	No	S	NA	6222:1
P	Yes	S	89.3%	659:1
P	Yes	P	91.3%	164:1
S	Yes	S	92.1%	82:1

Temporal waveforms obtained for the gate with crossed polarizers, as registered in different channels of the oscilloscope, are shown in Figure 3. The "optimized" drive voltage waveform to the LCR, corresponding to the orange curve, is being repeated at the 2 kHz rate of SLR2000. The purple curve, corresponding to the optical detector output, is a good approximation to the "ideal" transmission waveform in Figure 1, where the gate is closed for 50 microseconds and open for 450 microseconds and shows a fast transition between the two states (< 10 microseconds). The upper green curve is the purple curve viewed at high resolution and clearly shows the rapid reversal in the transmission trend as the drive waveform voltage to the LCR changes sign.

It is worthwhile to point out certain required characteristics of the drive waveform. The integral of the waveform over one cycle must equal zero, i.e. the positive area under the waveform must equal the negative area. If the average is not zero, any ions present in the liquid crystal will migrate to the surfaces resulting in a build-up of charge. This will effectively keep the liqud crystal pinned in that state [Bauchert, 2004]. Furthermore, during the "open" mode, one must apply a slight residual positive voltage (~2 to 3V) which holds the molecules in their transmissive state and prevents them from becoming randomly oriented and thereby reducing the transmission when the switch is "open". The width of the blocking gate is determined by the combined widths of the positive and negative going pulses. Because of the zero integral

condition over the full 500 microsecond cycle, the temporal width of the negative drive pulse is necessarily less than that of the positive pulse.

Integration into SLR2000

Figure 4a shows the current SLR2000 receiver configuration where the incoming light is split into s and p polarizations and then recombined on a final polarizer before impinging on the quadrant MCP/PMT. Note that, without the LCR, the polarization of the light is preserved during recombination at the final polarizer. Thus, using the results in Table 2 for uncrossed polarizers, one can project a mean transmission of 91.7% for the open gate and a mean extinction of 123:1 for unpolarized light entering the receiver. Significantly better performance is obtained if a mirror is placed to the left of the combining polarizer as in Figure 4b and the drive voltages to the LCR are reversed. The expected extinction rises significantly to 659:1, and the transmission decreases only slightly to 89.3% for unpolarized input.

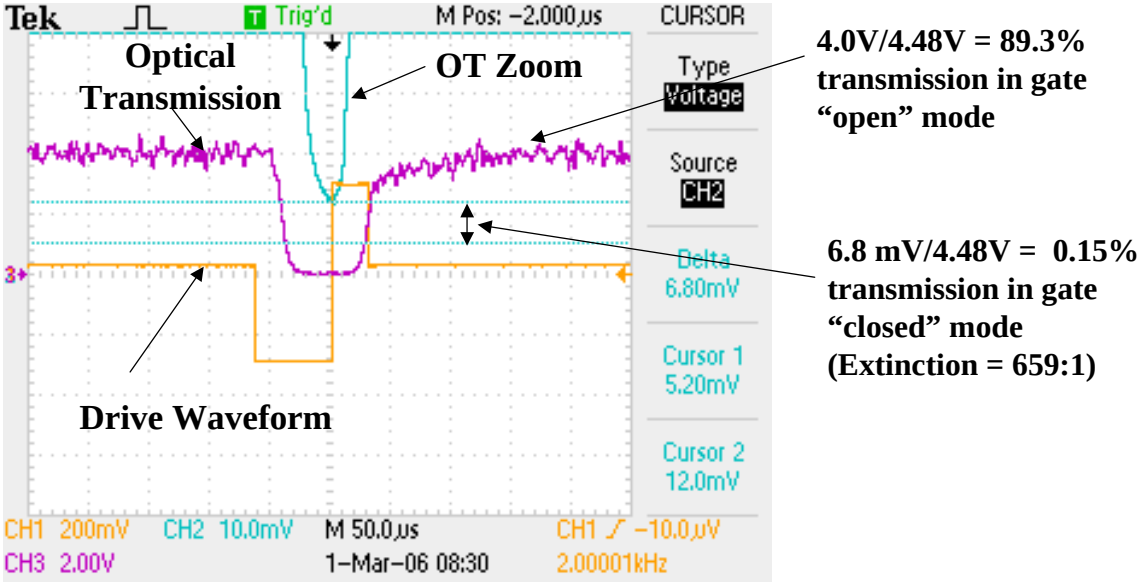

Figure 3: *Oscilloscope traces obtained during transmission/extinction experiments with the normal crossed polarizer configuration. The drive waveform to the LCR is indicated by the orange trace. The purple trace gives the optical transmission from "open" to "closed to "open". The narrow green trace at the top of the figure is a high vertical resolution version of the purple trace and shows the rapid reversal in the optical transmission trend at the point where the sign of the applied LCR voltage is suddenly reversed.*

Summary

We have demonstrated that liquid crystals, when used as a 90^{o} polarization rotator between two cube polarizers, can:

- reduce the amount of laser backscatter by 2 to 3 orders of magnitude in the "closed" state while exhibiting high transmission (~90%) in the "open" state,
- operate at few kHz rates,
- handle large aperture beams (~15 mm),
- switch states in less than 10 microseconds with low voltage (<$\pm$30V),
- produce flexible gate waveforms of arbitrary shape and duration,
- work in tandem with variable laser fire rates to avoid "collisions" between incoming and outgoing pulses.

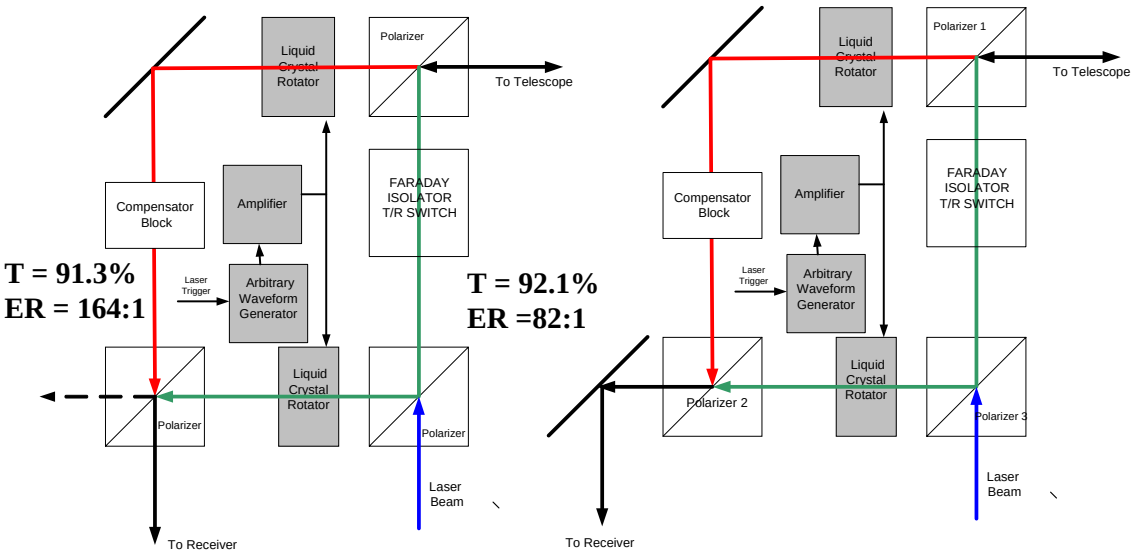

Current SLR2000 Configuration Uncrossed Polarizers (average)	Better Configuration Crossed Polarizers
T = 91.7% ER = 123:1	T= 89.3% ER = 659:1

Figure 4: *(a) With LCR's installed in both legs of the current SLR2000 receiver and unpolarized signal, the mean transmission and extinction would be 91.7% and 123:1 respectively; (b) a minor modification of the SLR2000 receiver configuration would result in 89.3% transmission and 659:1 extinction.*

We close with certain precautions in the use of these devices. The liquid crystal medium is sandwiched between two optical substrates. Care must be taken when mounting the LCR's to avoid stressing the delicate interface. The voltage to the unit must not exceed the $\pm$ 30VDC maximum or serious damage to the interface may result. Also, as mentioned previously, in designing the drive waveform, the voltage over one repetition cycle must average to zero.

References

[1] Bauchert, K., Boulder Nonlinear Systems, private communication, 2004.

[2] Degnan, J., "Ray Matrix Approach for the Real Time Control of SLR2000 Optical Elements", Proc. 14th International Workshop on Laser Ranging, San Fernando, Spain, June 6-10, 2004.

SLR 2000: The Path toward Completion

J. McGarry, T. Zagwodzki

1. NASA / Goddard Space Flight Center.

Contact: Jan.McGarry@nasa.gov

Abstract

After years of programmatic and technical issues, SLR2000 is finally receiving the manpower and money needed to solve the final technical challenges. This paper describes the progress that has been accomplished over the past year and discusses the final steps that we will take in the coming year to make the system operational.

Introduction

SLR2000 is the prototype for NASA's Next Generation of Satellite Laser Ranging (SLR) Systems. It was originally designed to be completely automated, eye-safe, with a lower cost of operation, a high reliability, and an accuracy comparable to the existing NASA MOBLAS systems [Degnan(1)]. After many years where funding was low, in 2006 SLR2000 development was given a higher priority and more funding.

Much progress has been made in the last year. The system is now tracking low earth orbiting (LEO) and LAGEOS satellites, able to acquire and track most LEOs relatively easily, although the returns are not yet optimized. The system timing, pointing and ranging capability, and accuracy have been tested using MOBLAS-7 return pulses. The software is more robust and the system is more repeatable. We believe that the system is within a year of final collocation with MOBLAS-7.

Recent system developments.

An optical shutter was designed and built by SigmaSpace and installed in the system to reduce the laser backscatter on the detector [Degnan(2)]. In a single telescope common optics transmit-receive system the photomultiplier tube (PMT) is exposed to a significant amount of laser backscatter within its field of view (FOV) as the pulse leaves the system. Even though the PMT is gated off during the laser fire this illumination stresses the photocathode and may shorten its lifetime. Mechanical choppers or shutters were investigated but deemed too problematic for operation at 2 KHz. The solution was an optical shutter in the form of two liquid crystal (LC) polarizing filters, one installed in each leg of the transmit-receive switch which reduce the backscatter by two orders of magnitude (Figure 1).

A new higher quantum efficiency (QE) quadrant PMT was installed in the system. The comparison with the previous detector is shown in the following table.

	Photek(PMT210)	Ham(R4100U- 74-M004C)
MCP stages	2 plates	2 plates
Active diameter	10mm	6mm
Photocathode	S20	GaAsP
Q.E.*	12%	33%
DC current Gain	1×10^6	2.6×10^5
PMT HV bias	-4700V (nom.)	-2250V (nom.)

The relative sensitivity improvement of the Hamamatsu tube over the Photek tube was estimated during an Etalon track to be approximately 5:1. Additional loss in Photek

sensitivity is surmised to be due to aging or degradation of the photocathode over many months of SLR operation.

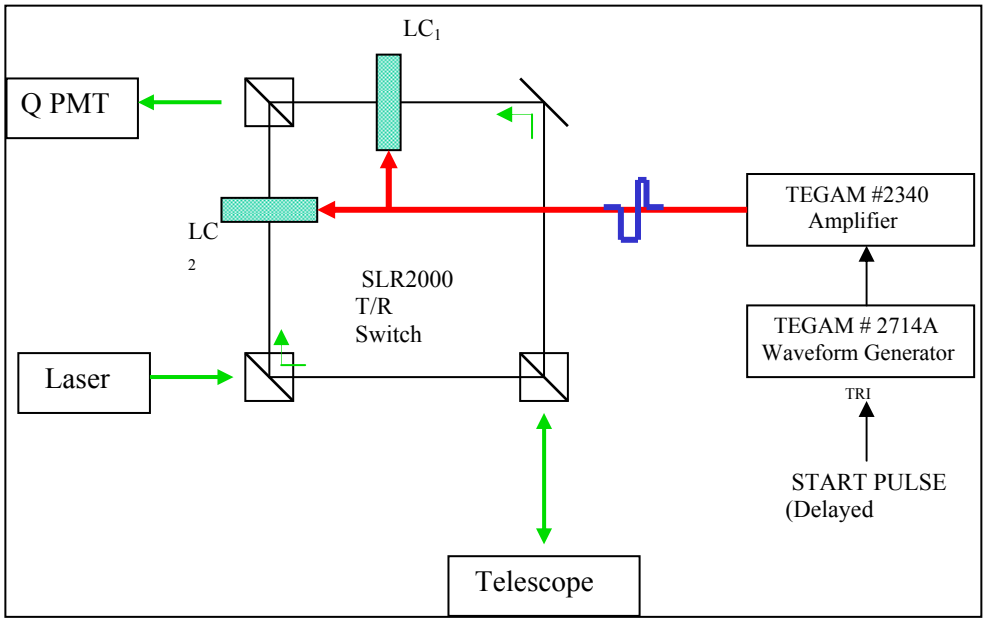

Figure 1: *Optical bench with Liquid Crystal Shutter in both legs of T/R switch*

A laser beam expander was replaced in the system to both control the laser divergence and to give adequate knowledge of the divergence setting. This expander was designed and built by SigmaSpace [Degnan(3)]. Originally the laser transmitter beam divergence could not be adjusted without de-focusing the common beam expander for the receiver. The resultant FOV change in the receiver adversely effected control of background noise and vastly complicated tracking. The solution was to develop a beam expander mechanism which operates solely on the laser transmit beam (independent of the receive path) and which could be focused to accommodate the 10 to 30 arcsecond (full angle) desired beam width.

The Risley prism laser point-ahead optics are now operational in the system [McGarry]. The Risley wedge pair is used to steer the transmit beam ahead of the telescope receive path and put the center of the transmit laser beam directly on the target. The telescope can then be pointed behind to center the receive FOV about the return light. This then allows the FOV to be closed to 10 arcseconds, which reduces the optical noise and allows use of the quadrant detector information to correct the telescope pointing. The Risley optics have successfully undergone testing with an off-line software package. The operational software package interface to the Risleys will be verified in the next few months.

The software now controls the Laser Pulse Repetition Frequency (PRF) to avoid fire/return collisions [Titterton]. This is needed due to the common optics design of the system. Only two different fire intervals are needed for any of the ILRS tracked satellites. The values of the two fire intervals are dependent upon altitude:

- Low Earth Orbiting (LEO): 500 and 510 microseconds
- LAGEOS: 500 and 502 microseconds
- High Earth Orbiting (HEO): 500 and 501 microseconds

The PRF switching is currently being successfully used in all satellite ranging. Figure 2 shows how the laser PRF changes during the course of a LEO (left plot) and LAGEOS (right plot) pass.

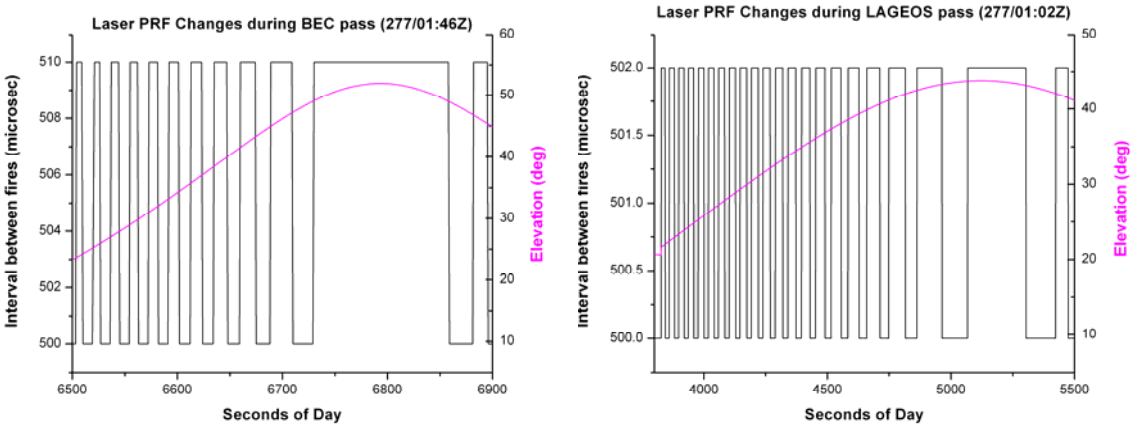

Figure 2: *Examples of laser PRF changes during two passes. The left plot is BEC and the right plot is LAGEOS.*

The new Q-Peak laser was installed into the system. The energy of the previous laser (an earlier Q-Peak version) had degraded to the point where it was transmitting only about 60 microJoules per pulse. The newer laser transmits approximately 120 microJoules per pulse.

Both the star camera (for star calibrations) and the sky camera (for sky condition) failed during 2006 and have been replaced. The star camera had been in use for approximately ten years. The new star camera is the Santa Barbara Instrument Group (SBIG) ST-402ME CCD imaging camera. The CCD chip is 9 microns square with 765 x 510 pixels. It is a low noise, high QE camera with a USB 2.0 interface. It greatly increases the star sensitivity from our old camera, where the dimmest useable star was around magnitude 3.5. The SBIG camera in SLR2000 can resolve better than 8th magnitude stars. The new star camera has been installed and is operational.

The sky camera failed after about five years of more or less continuous operation. The new sky camera is the Jenoptik VarioCam InfraRed (8 – 13 μm) camera. It has an uncooled sensor with a 320 x 240 pixel resolution and a Fire-Wire interface. The new sky camera is installed and working but has not yet been incorporated into the operational software.

Testing with MOBLAS-7

To checkout the system timing, pointing and receive electronics, we took many passes with MOBLAS-7 acting as the transmitter for SLR2000. These tests took two forms: (1) transferring the receive time from the MOBLAS-7 discriminator to the SLR2000 event timer with a cable running between the systems (start/stop via cable), and (2) receiving the actual return light with the SLR2000 quadrant detector. In both cases the MOBLAS-7 fire time was transferred to SLR2000 via cable.

Analysis showed (1) good pointing for SLR2000 (these tracks required no biases to maintain the returns), (2) comparable results between MOBLAS-7 and SLR2000 for data RMS when the cable was used to transfer the MOBLAS-7 fire times, and (3) in general a higher return rates for HEO satellites at SLR2000, due to its singe photon detection capability. Examples of the full rate data RMS for various passes are given in the table below.

Figure 3 shows an example of the LAGEOS return rates for MOBLAS-7 and SLR2000 with MOBLAS-7 providing the fires for both systems and SLR2000 receiving the return light with the quadrant detector.

LAGEOS RMS (mm)
MOBLAS-7 Start/Stop via cable: 10
SLR2000 quadrant detector: 25 – 40
ERS-2/ENVISAT RMS (mm)
SLR2000 quadrant detector: 20 – 25
GLONASS-87 RMS (mm)
MOBLAS-7 Start/Stop via cable: 15
SLR2000 quadrant detector: 35 - 45
ETALON RMS (mm)
SLR2000 quadrant detector: 50 – 60

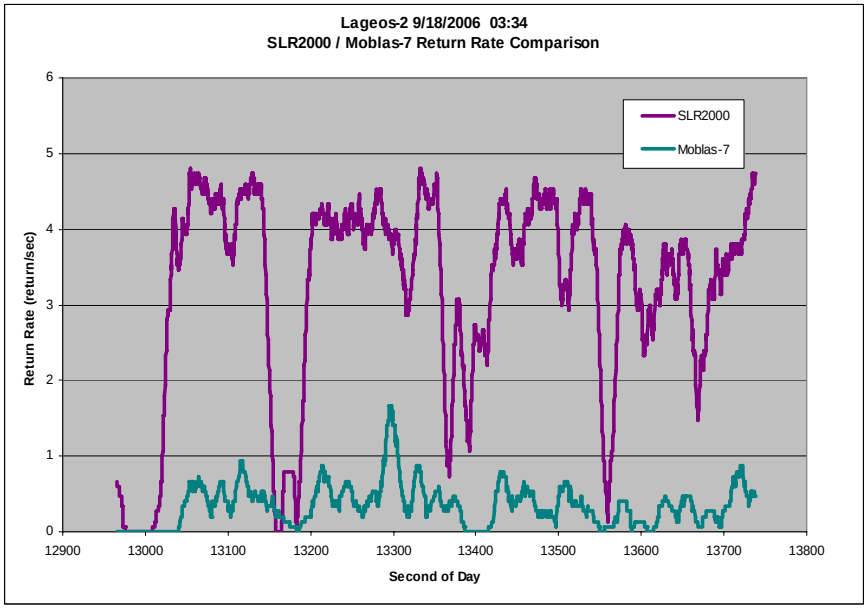

Figure 3: *LAGEOS return rates for SLR2000 (top curve) and MOBLAS-7 (bottom curve) when MOBLAS-7 was used as laser transmitter (5Hz) for both systems.*

Satellite ranging with the 2 kHz eyesafe laser

In the last several months SLR2000 has been ranging to satellites using its own eye-safe 2 kHz laser and pointing the telescope ahead. This configuration removes the need for the Risleys to point the laser ahead, but prevents daylight operation due to the need to keep the receiver field of view open to 25 arcseconds to cover the point-behind angular deviation from the point-ahead.

We have tracked many low earth orbiting satellites as well as a portion of a few LAGEOS passes. The pass RMS values remain relatively high due to our relatively wide pulse width laser (250 picoseconds). An example of the raw data from a STARLETTE pass is shown in Figures 4.

Path to Completion

Our immediate goal for 2007 is to increase our return rate from LAGEOS when ranging with our 2 khz eye-safe laser. We also need to return to our operational configuration where the telescope is pointed behind (toward the receive light) and the Risleys are used to point the laser ahead of the target. In this configuration we will work on finishing the closed-loop tracking. We expect our return signal rate to increase measurably when the system is closed-loop tracking.

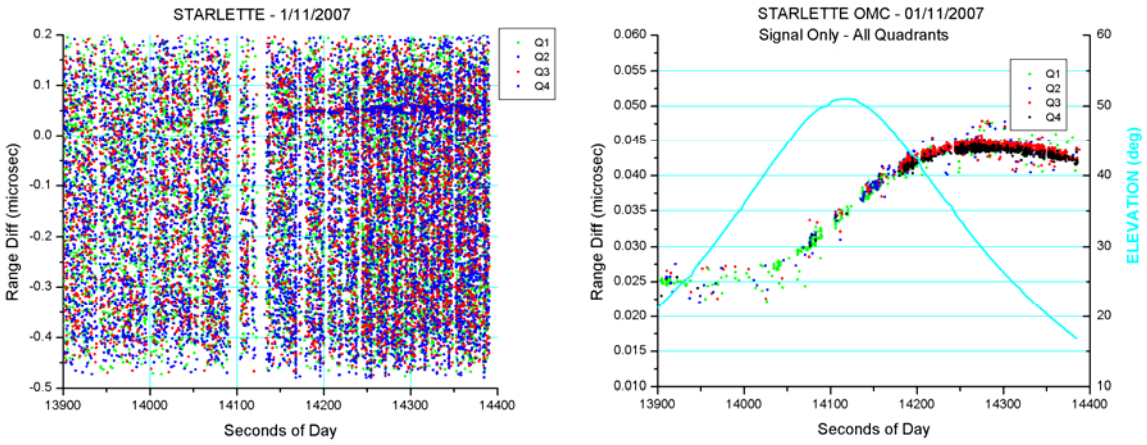

Figure 4: *STARLETTE pass on 1/11/2007. Left plot shows entire range window with signal and noise. Right plot is of signal only (as determined by signal processing).*

Along with this work, a new in-house laser is being built by Barry Coyle and colleagues. This 2 khz laser is expected to have a less than 200 picosecond pulse width with a 100 microJoule to 2 milliJoule variable per pulse output energy. This laser, which will enable us to track the higher satellites (in particular GPS), is expected to be delivered near the end of 2007. Our goal is to complete the SLR2000 prototype system in calendar year 2007 and perform a collocation with MOBLAS-7 in early 2008.

Acknowledgements

The authors would like to thank John Degnan, who developed the concept of SLR2000 and who led the development of this system until recently, for both his original idea and for his continued and unfailing support of this effort. We would also like to thank the SLR Network Manager, David Carter, for his support of our work, and Michael Pearlman who, as chairman of the ILRS Central Bureau, has been a steadfast proponent of SLR2000. We would also like to acknowledge the SLR2000 team, whose efforts were instrumental in SLR2000's progress: Christopher Clarke, John Cheek, Peter Dunn, Howard Donovan, Mike Heinick, Julie Horvath, Anthony Mallama, Anthony Mann, Donald Patterson, Mike Perry, Randall Ricklefs, Mark Torrence, Susan Valett, and Thomas Varghese. This work is being performed with funding from NASA's Science Mission Directorate.

References

[1] Degnan, J., J. McGarry, and T. Zagwodzki, "SLR2000: An Inexpensive, Fully Automated, Eyesafe Satellite Laser Ranging System," Proceedings of 10th International Laser Workshop on Laser Ranging Instrumentation, Chinese Academy of Sciences, Yang Fumin (ed.), 367-377, Shanghai, 1996.

[2] Degnan, J., and D. Caplan, "Performance of Liquid Crystal Optical Gate for Suppressing Laser Backscatter in Monostatic Kilohertz SLR Systems", in this Proceedings.

[3] Degnan, J., G. Jodor, and H. Bourges, "Adaptation of a Commercial Beam Expander for Automated Transmitter Beam Size and Divergence Control in the SLR2000 System", in this Proceedings.

[4] McGarry, J., T. Zagwodzki and J. Degnan, "SLR2000 Closed Loop Tracking with a Photon-Counting Quadrant Detector," Electronic Proceedings of 13th International Workshop on Laser Ranging, Ron Noomen (ed.), Automation and Control Session, Washington, DC, 2002.

[5] Titterton, P., H. Sweeney, and D. Leonard, "System/Usage Impact of Operating the SLR2000 at 2 kHz," Proceedings of the 11th International Workshop on Laser Ranging, 426 – 437, Deggendorf, 1998.

Determination of AJISAI spin parameters using Graz kHz SLR data

Georg Kirchner, Walter Hausleitner, and Elena Cristea

1. Austrian Academy of Sciences, Institute for Space Research, Graz.

Contact: Georg.Kirchner@oeaw.ac.at ; Walter.Hausleitner@oeaw.ac.at ;
Elena.Cristea@oeaw.ac.at

Abstract

Using the Graz full rate kHz SLR data, we determined the spin rate and spin direction of the satellite AJISAI as well as its slow down between 2003/10 and 2005/06. The high density of the kHz data results in a precise scanning of the satellite's retro-reflector panel orientation during the spin motion. Applying spectral analysis methods, the resulting frequencies allow identification of the arrangement of the involved laser retroreflector panels at any instant in time during the pass. Using this method, we calculated the spin rate with a high accuracy (RMS of 4.03 x·10^{-4} Hz), and the slow down of the spin rate during the investigated period with a magnitude of 0.0077497 Hz/year. We obtained these results from routine SLR tracking data, i.e. day and night observation, without any additional hardware.

Introduction

The Japanese geodetic satellite AJISAI, launched on August 13, 1986 into a 1500 km circular orbit with a 50° inclination, is a passive sphere with a diameter of 2.15 m [1]. The surface is covered with 318 sunlight reflection mirrors for visual tracking and 120 laser retro reflector (LRR) panels each carrying 12 corner cube reflectors for SLR [2] (see Fig. 1). The satellite's axial rotation causes the mirrors to produce visible flashes of reflected sunlight, which are observable on Earth [4]. This in principle allows a precise determination of the spin rate, but, however, requires dedicated photometric equipment at the ground station. Furthermore, these observations can only be made during night time, and for limited time spans where the satellite is illuminated by the Sun. This method was applied for AJISAI in Japan only in the frame of a few campaigns.

AJISAI was put into orbit with an initial spin rate of 40 rpm, and with the spin axis parallel to the Earth's rotation axis. With the method of photometric timing an axial rotation of 0.67 Hz was measured after launch [5], slowing down to 0.57 Hz by October 1997 [2].

In the present study AJISAI's spin rate has been investigated using the full rate kHz SLR observations of the Graz laser station and was determined to be 0.5064 Hz in July 2005. The main reason for this slowdown is the eddy current resulting from an interaction between the satellite's metallic parts and the Earth's magnetic field [2].

While standard SLR measurements are usually done at a 5 or 10 Hz repetition rate, the SLR station Graz was upgraded and is operating a 2 kHz laser system since October 2003. Due to the capability of detecting return pulses with as few as a single photon, the return rate from AJSAI comes close to 100 %, even with the low energy per shot 400 µJ) of the Graz SLR system. The 2 kHz repetition rate produces up to 1 million measurements per AJISAI pass, which has a duration of typically 16 minutes. This amount of data represents a very dense temporal sampling of the satellite's rotating surface, which allows an accurate determination of the spin parameters.

Fig. 1. *Geodetic satellite AJISAI.*

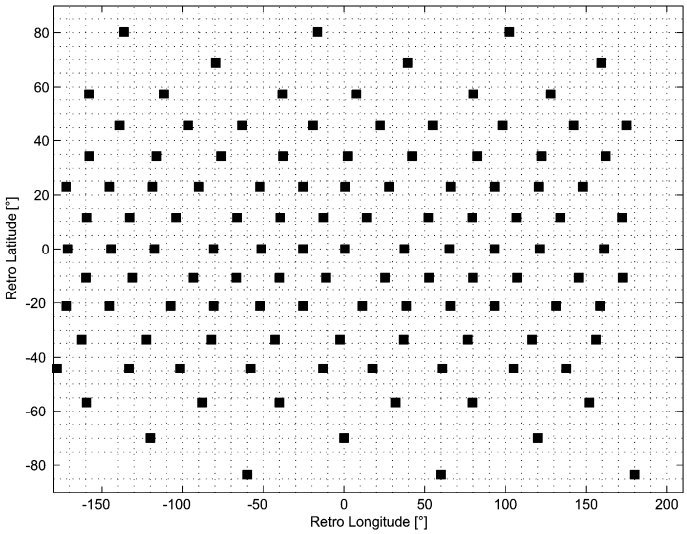

Fig. 2*. Schematic distribution of the LRR panels*

The LRR panels are almost uniformly distributed over the surface, arranged in 15 latitudinal rings [2]. There are 5 rings with 12 LRR's, 4 rings with 9 LRR's, 2 rings with 6 LRR's, and 4 rings with 3 LRR's each. The schematic distribution of these LRR panels in terms of latitude and longitude is shown in Fig. 2.

Ranging Simulations

Due to the axial rotation of AJISAI and the well separated reflector panels, the distance from the observer to each panel varies periodically. The periods are given by the spin rate of the satellite and the number of panels of the involved ring. The amplitudes depend on the dimension of the sphere, the distance between the panels and on the incidence angle of the laser beam. Based on the known location of each reflector panel on AJISAI [6], a ranging simulation was made which clearly shows the expected periodic distance variation.

Fig. 3 shows a full 360° rotation viewing with an incident angle of –18.125° from the satellite's equator, which contains 12 reflector panels, consisting of 3 groups with 4 panels each. The distances between these 3 groups are slightly larger than the distances between the panels within each group (Fig. 2). The resulting pattern shows the corresponding peaks, with 3 larger gaps (at 100°, 220° and 340° longitude) in between.

Spectral analysis of kHz data

In order to verify these simulation results, using the Graz kHz SLR measurements, we calculated a reference orbit from the standard SLR predictions and subtracted the calculated value from the measured distance. A low order polynomial was approximated and subtracted from the residuals in order to remove the remaining low-frequency part (approx. a few minutes in time) of the observations, but keeping the high-frequency variations (less than a few seconds) originating from the rotating reflector panels.

Fig. 4 shows range residuals for a 2 s interval (1 full revolution) of a routinely observed AJISAI pass.. The residual plot clearly shows the bigger gaps (longer ranges) due to the larger distances between the 3 groups as well as small variations in

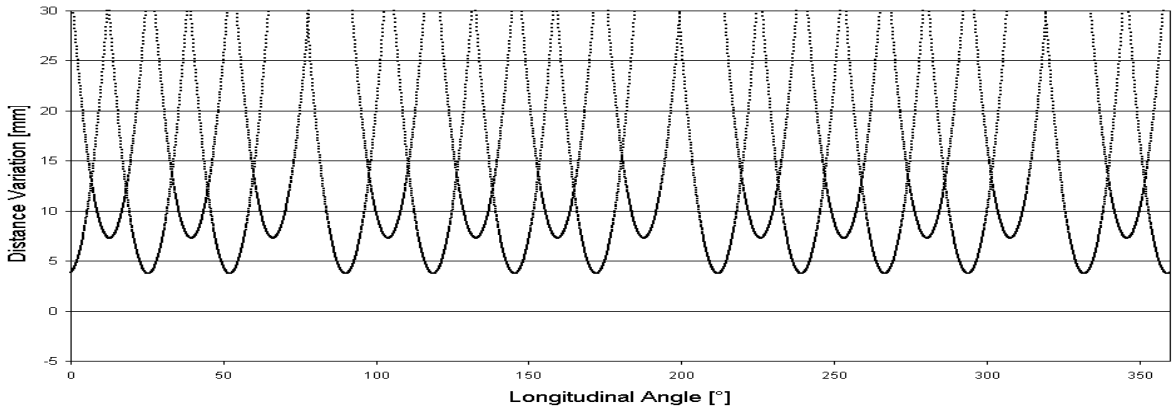

***Fig. 3**. Simulated distance variations of LRR panels at a laser beam incidence angle of -18.125° latitude. The non-symmetric LRR arrangement (Fig. 2) causes the slightly irregular distribution in both the simulation (Fig. 3) and in the ranging residuals (Fig. 4).*

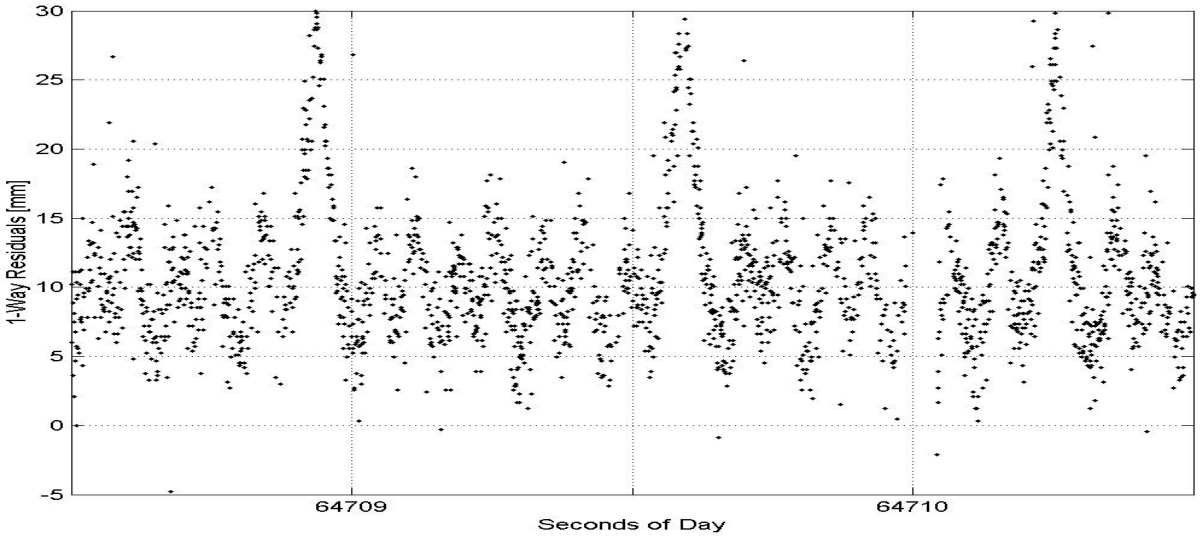

***Fig. 4**. Full rate 1-way range residuals during one full rotation of AJISAI (DOY 122/2005) for comparison with the simulation shown in Fig. 3*

between due to 2 different rings. This residual analysis coincides well with the corresponding simulation shown in Fig. 3.

Frequency Analysis using FFT versus Lomb

Usually, SLR systems do not reach a 100 % return rate, even in good weather conditions. Due to the resulting gaps, the measurements are in general not equidistant in time and therefore the Fast Fourier Transform (FFT) method cannot be directly applied for a frequency analysis. In order to use FFT for the given AJISAI range residuals, the data gaps may be interpolated, but, however, this may induce new frequencies and decrease the accuracy of the results [8]. In [2], the Lomb method for spectral analysis of non-uniformly distributed data was suggested as a useful alternative. This method can handle non-equally spaced data and provides an approximation of the spectrum using the least-squares method.

Connecting Frequencies with AJISAI Geometry

Applying the Lomb method to the residuals of a 10 seconds interval of an AJISAI pass (see Fig. 5), a number of spectral peaks due to the distance variations can be seen clearly. The frequencies of 1.5, 3.1, 4.6 and 6.1 Hz are multiples of AJISAI's basic

spin rate of about 0.5105 Hz in January 2005, and the number of LRR panels (3, 6, 9 or 12) of the involved ring. The higher frequencies of 7.57, 9.09, 10.60 and 12.12 Hz are generated by simultaneous contributions of LRR of two or more adjacent rings. For instance, the clear spectral peak at 12.12 Hz in Fig. 5 cannot be associated with any single ring, but is produced by the combination of two 12-retro rings.

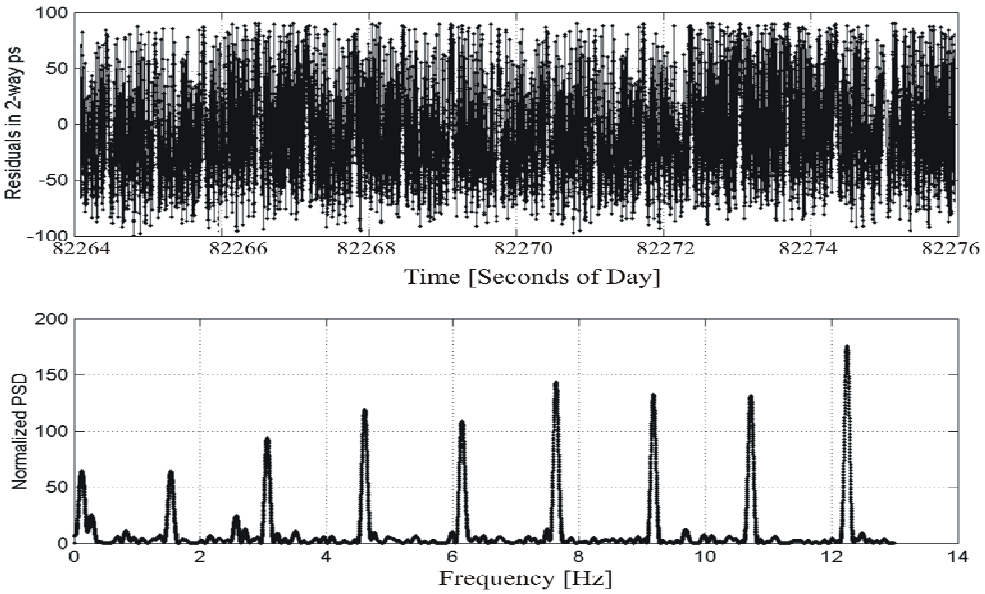

Fig. 5. *Twelve seconds interval of 2-way residuals in time and frequency domain (DOY 019/2005, multiple rings visible).*

Spin rate slow down

It was shown that each calculated frequency corresponds to a specific number of LRR panels. The ratio between frequency and the number of panels of the corresponding ring gives the exact spin rate of AJISAI. The frequency generated by the 3 LRR rings was not used for spin rate calculations, because they generate lower spectral power and lower resolution than the 6, 9 or 12 LRR rings.

For the frequency analysis we selected only passes with high data density (> 300 k returns) observed between 2003/10 and 2005/06. From these passes we used only data of a 1.5 minutes interval centered at the closest approach, containing more than 40 k returns, in order to keep the computation time within reasonable limits (a 3 GHz PC still needed 5 days to analyze the 195 selected passes).

Because the measured spin rate is an apparent spin rate it was corrected for the apparent effect in order to get the sidereal spin rate (see details below). The resulting spin rates for this time span show a well defined slow down rate of 0.0077497 Hz / year (Fig. 6), coinciding well with AJISAI's spin rate slow down calculated for 1997-1999 [2].

Apparent Spin and Spin Direction

The apparent spin rate of a satellite observed at any site on Earth is affected by the axial spin as well as by its orbit around the Earth and by the Earth rotation itself. Therefore the apparently measured spin has to be corrected for these effects, in order to obtain the sidereal spin of AJISAI.

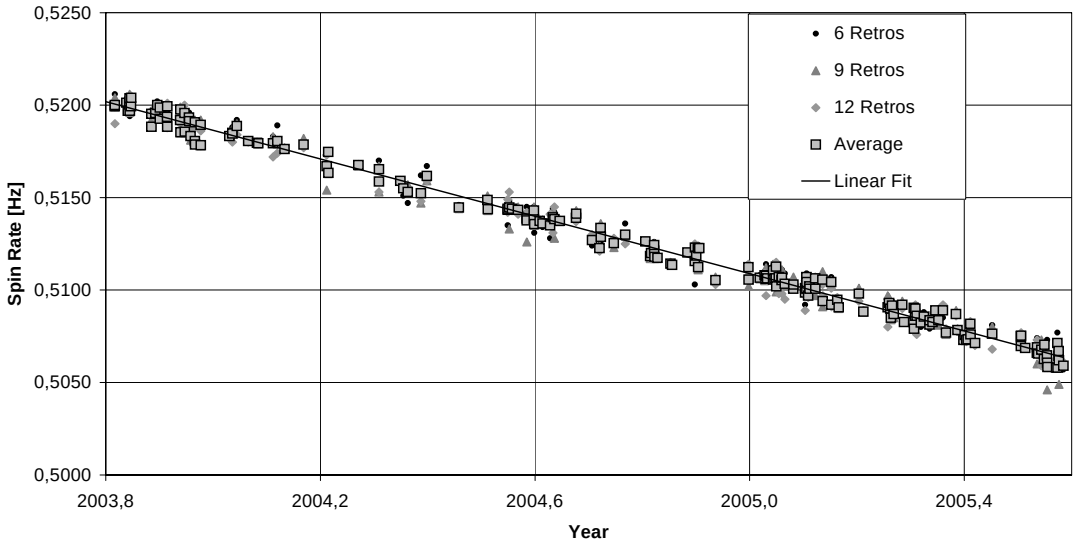

Fig. 6. *AJISAI spin rate decrease determined from the averages of 6, 9 and 12 retro ring spin rates for 195 passes between 2003/10 and 2005/06. The linear fit to these average values yields a slow down rate of 0.0077497 Hz / year, with a standard deviation of 0.000403 Hz.*

As an example, we calculated the spin rate of an AJISAI pass of 2005/01/19 (again for a period of 1.5 minutes around the closest approach). However, in this case, we selected only short slots of 12 seconds (containing at least 5000 residuals), calculated the spin rate with the same approach as above, then shifted the slot time by 6 seconds, and repeated the procedure.

This results in a clearly visible – apparent – increase of the spin rate near the maximum elevation (71.9° for this pass) as shown in Fig. 7, where the values are given together with the corresponding calculated apparent spin rate. The clearly visible outliers at about 82050, 82150 and 82250 seconds can be correlated with according ring transitions, identifiable by detailed analyses of the residuals. The results confirm the high sensitivity of kHz SLR data for the determination of satellite spin rates.

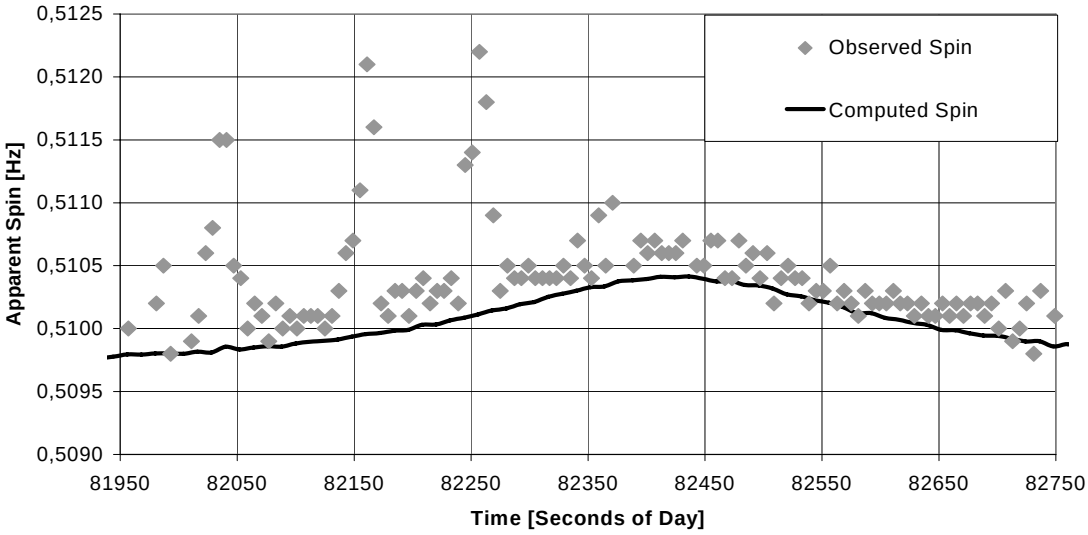

Fig. 7. *Apparent spin motion as observed from the SLR site. Measured rates (diamonds) vs computed values (solid line).*

We assume that the spin direction of AJISAI a priori is not known. From sequences of observed LRR ring transitions in most passes we have evidence that the spin axis is still at least approximately parallel to the Earth axis. Because the closest approach (CA) of the selected pass was at about 160° / 71.9° (as seen from Graz), and the apparent spin shows a slight increase (Fig. 7) at CA, we can conclude that AJISAI is spinning in a clockwise direction.

References

[1] T. Otsubo, J. Amagai, and H. Kunimori, "The center of mass correction of the geodetic satellite AJISAI for single-photon laser ranging", IEEE Transactions on Geoscience and Remote Sensing, Vol. 37, No. 4, July 1999.

[2] T. Otsubo, J. Amagai, H. Kunimori, and M. Elphick, "Spin motion of the AJISAI satellite derived from spectral analysis of laser ranging data", IEEE Transactions on Geoscience and Remote Sensing, Vol. 38, No. 3, May 2000.

[3] International Laser Ranging Service (ILRS) Home Page: http://ilrs.gsfc.nasa.gov .

[4] R. Wood, T. Otsubo and R. Sherwood, "Lageos 2 spin rate and orientation", http://cddisa.gsfc.nasa.gov/lw13/docs/papers/target_wood_1m.pdf

[5] T. Kanazawa, "Determination of the rotation phase angle and the rotation period of AJISAI(II)" in Proc. 70th meeting Geodetic Soc. Of Japan, Kyoto, Japan, 1988, pp. 51-52.

[6] T. Uchimura, Personal communication, July 2005, (uchimura.takashi@jaxa.jp)

[7] M. Sasaki and H. Hashimoto, "Launch and observation program of the experimental geodetic satellite of Japan", IEEE Transactions on Geoscience and Remote Sensing, Vol. GE-25, No. 5, September 1987.

[8] N. R. Lomb, "Least-squares frequency analysis of unequally spaced data", Astrophysics and Space Science 39, p. 447-462, 1976.

New Methods to Determe Gravity Probe-B Spin Parameters using Graz kHz SLR Data

Georg Kirchner, Daniel Kucharski, Elena Cristea

1. Austrian Academy of Sciences, Institute for Space Research, Graz.

Contact: Georg.Kirchner@oeaw.ac.at ; Walter.Hausleitner@oeaw.ac.at ;
Elena.Cristea@oeaw.ac.at

Abstract

Using kHz data of the SLR station Graz, spin parameters of the satellite Gravity Probe B (GP-B) are derived; these include spin period and its change over a 1.5 year period, as well as spin direction, and spin axis orientation. The results are compared to the actual data sets - as determined by the GP-B mission itself – thus allowing independent confirmation of the kHz SLR derived results.

Introduction

GP-B was launched on April 20th, 2004, into a polar orbit at 640 km altitude. During its measurement phase, the spacecraft was spinning slowly - with about 77.5 seconds / revolution - around its central axis, defined by a telescope at one end, and the laser retro reflector (LRR) array at the other end. Its orientation was maintained always to point with high accuracy to the star IM-Pegasus; the direction to this star is measured with the on-board telescope with a stability of 0.1 milliarcseconds per year [1] (ed.).

The LRR array (Fig. 1) on GP-B consists of 8 retro reflectors in a ring-like formation, and a central LRR [2]. While such an arrangement only spreads standard SLR measurements, the high resolution of kHz SLR allows to scan the single reflectors, to identify their motion due to the spin of the satellite, and to derive all GP-B spin parameters from kHz SLR data.

Spectral Analysis of kHz Slr Data

The spectral analysis of kHz SLR data is based on residuals obtained by subtracting the calculated, predicted orbit, from the measured distances. Fitting a low order polynomial to these residuals allows elimination of outliers, but keeps the oscillating signal of the eight rotating LRR's (Fig. 2, top).

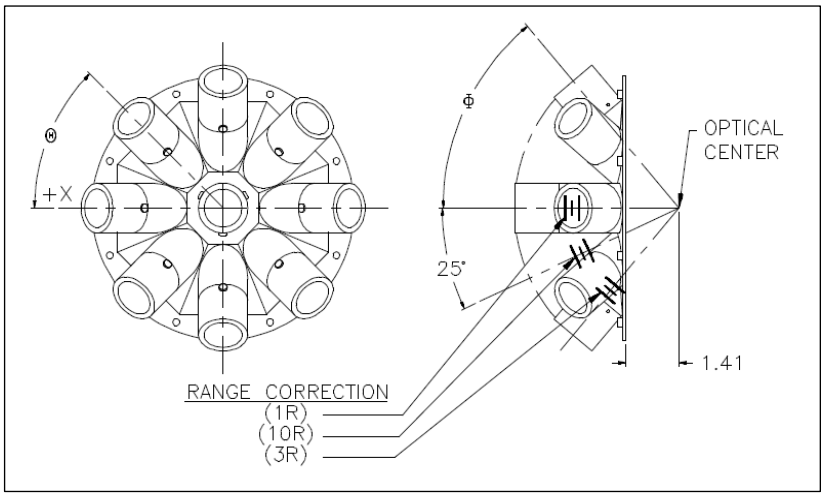

Fig. 1: *GP-B Laser Retro Reflector (LRR) Design*

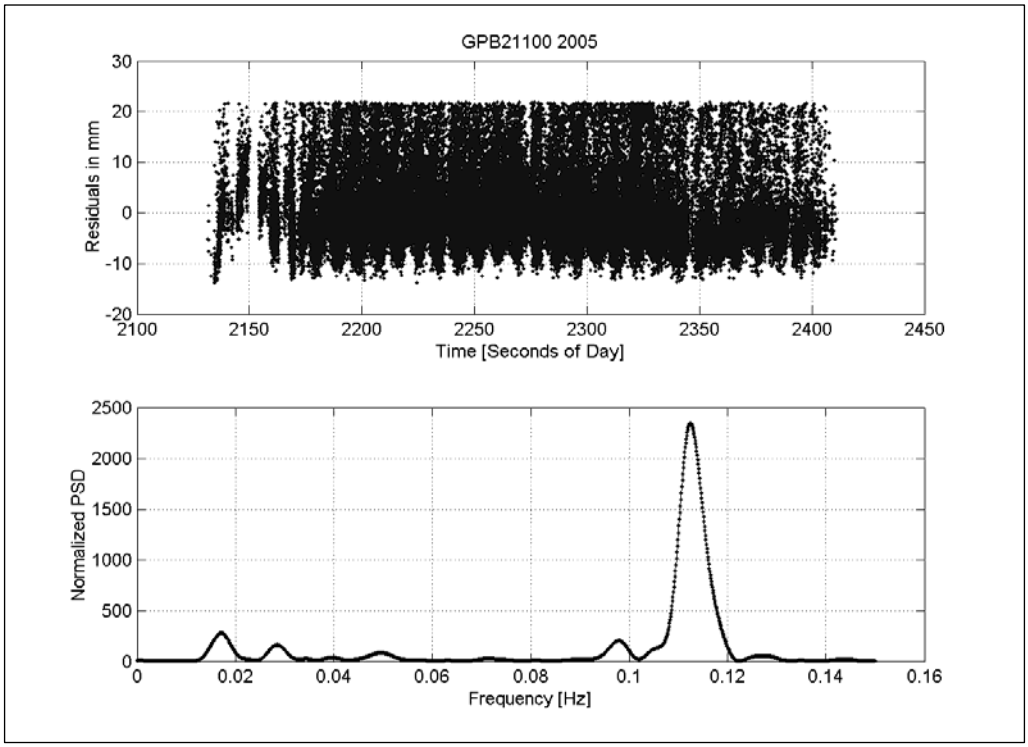

Fig. 2: *Residuals of a 280 seconds segment of a GP-B pass of DOY 211/2005 (top); frequency spectrum generated by these residuals (bottom).*

The Lomb method of spectral analysis was suggested in [3] alternatively to the Fast Fourier Transform (FFT), allowing for non-equally spaced data, as it is the case for such SLR measurements. The FFT could still be used if the data gaps were interpolated, but this would introduce unwanted frequencies. Therefore the Lomb method was preferred.

Taking into account the known inertial spin period of GP-B (77.5 seconds per revolution) during phase A (Fig. 3), and the 8 retro reflectors per revolution, we selected passes with at least 100 seconds to analyze a minimum of 10 oscillations, to get reliable results for the spectral power (Fig. 2, bottom).

This spectral power varies from pass to pass, with the data gaps and the length of the pass being the main corrupting factors. The analysis has been performed also on selected intervals of the longer passes, with high data density, as an additional verification of the frequency obtained for the complete pass.

Spin Period Trend

From all GP-B passes measured by Graz kHz SLR, we selected those with more than 50,000 returns per pass. Applying the Lomb analysis to these passes, we found three different regions of spin periods after the initialization period, as soon as SLR measurements started (Fig. 3, top): phase A: from 10.08.2004 until 6.09.2005, the mean spin period was about 77.5 seconds; phase B: the spin period changed to about 125 seconds; after 11.01.2006 (phase C), the spin period analysis shows an unstable behavior, as expected after termination of the active phase of the GP-B experiments (Fig. 3, top). Comparing the SLR derived spin periods with the GP-B based data set for phase A (Fig. 3, bottom), the RMS of the differences is 4.99 seconds.

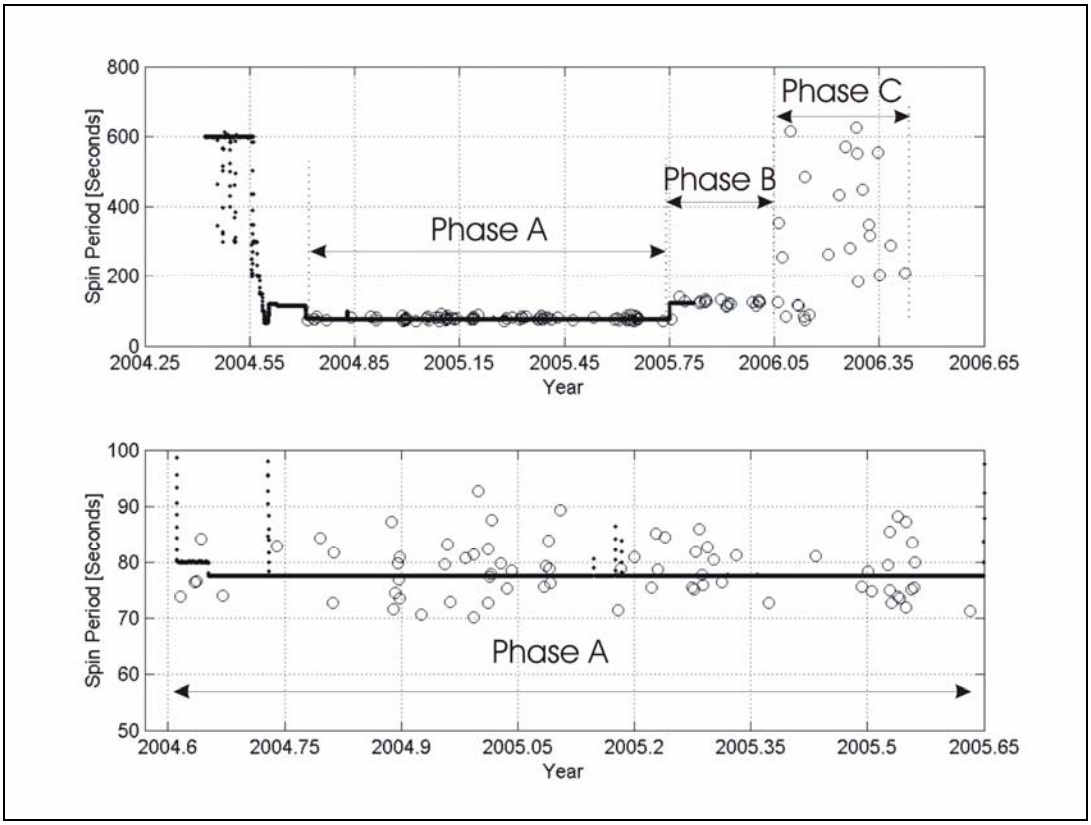

Fig. 3. *GP-B spin period variations. Dots indicate spin periods as measured on-board; circles (o) show results of kHz SLR spectral analysis. Bottom: Expanded view for phase A, showing RMS of 4.99 seconds.*

Apparent Spin

Although the spectral analysis already yields clear results – coinciding with the GP-B on-board measured data sets (Fig. 3) -, the accuracy is not as expected: the frequency peak (Fig. 2, bottom) is well defined, but rather broad; and the RMS of the differences between kHz SLR based periods and the on-board spin measurements (Fig. 3) amounts to rather high 4.99 seconds for phase A.

Simulating the measured GP-B passes, using all known parameters (GP-B orbit, Earth rotation, fixed pointing of GP-B to IM-Pegasus, inertial GP-B spin period as measured by the spacecraft itself, geometry of the retro reflectors, as well as their range corrections, etc.), the influence of the apparent spin - the satellite's spin as observed from Earth – was identified as the main reason (Fig. 4). GP-B's spin period is about 77.5 seconds; because the satellite moves along its orbit considerably during this time, the apparent spin period for even the short part (151 seconds) of the pass in Fig. 4 changes from initial 72.8 seconds (9.1 x 8 retro reflectors) to 70.4 seconds (as determined from peak-to-peak distances; Fig. 5). This change in apparent spin period is the main reason for the mentioned inaccuracies in the spectral analysis. In addition, the change of the incident angle of the laser beam causes a decrease of the "modulation depth", as indicated by the line in Fig. 4.

Spin Period Determination Using Simulation

Due to the low spin rate of GP-B, it is not possible to apply the apparent spin directly to the spectral analysis results, as it has been done in [4]; we therefore checked other

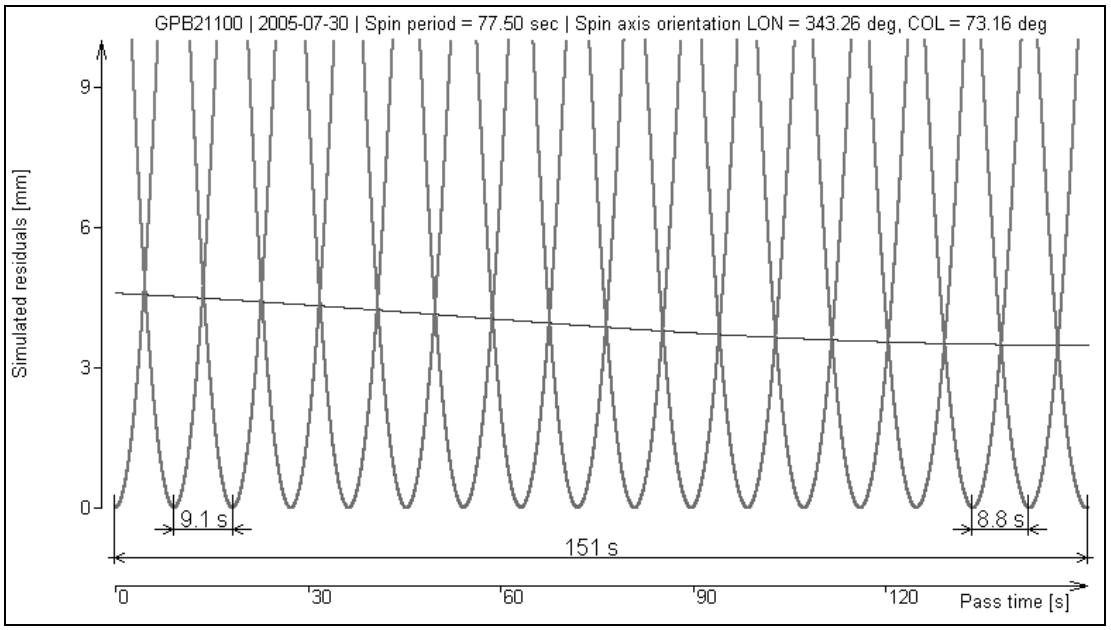

Fig. 4:. *Simulation of GP-B pass DOY 211/2005; spin period slightly changing due to apparent spin. The line shows the decreasing "modulation depth" during the 151 seconds.*

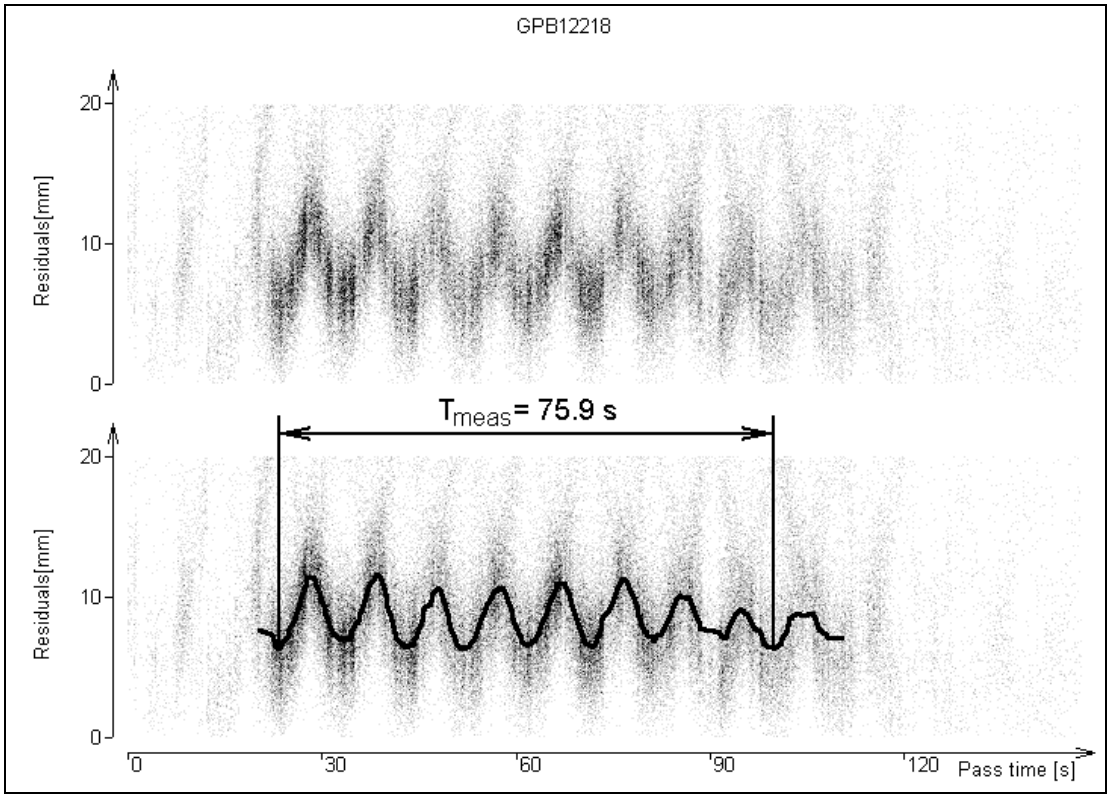

Fig. 5a: *GP-B pass of DOY 122 / 2005, Top: Residuals; about 79200 points in 151 s; bottom: solid line: averaging; 75.9 s from first to last peak (T_{meas}).*

methods to calculate more accurate, inertial spin periods for GP-B using our kHz SLR data.

The simulations, as described above, proved to be a good and powerful tool: for each measured pass, we determined the time period from first to last peak (Fig. 5a, T_{meas}); the same pass was simulated also (Fig. 5b, T_{sim}); however, the inertial spin period of

GP-B was used here as parameter, varying its value from –50 to –100 seconds, and from 50 to 100 seconds, in steps of 0.01 seconds. If the estimated and the true inertial spin periods coincide, the measured and the simulated T values for the same epoch times should be the same. In Fig. 6, the differences T_{meas} - T_{sim} for 100 phase A passes are plotted, allowing for both spin directions. The zero-crossings of these differences determine the inertial GP-B spin periods.

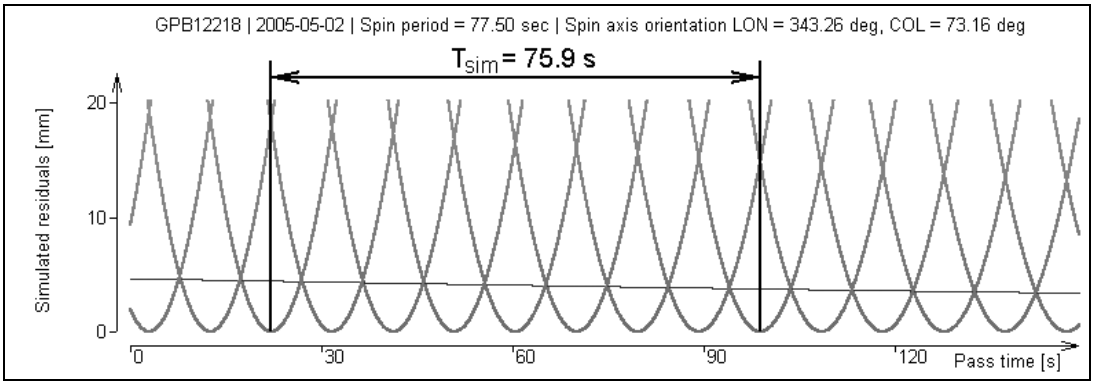

***Fig. 5b**: Simulation of same pass of DOY 122 / 2005: T_{sim} is same as T_{meas} at same epoch time, when simulating with inertial spin period of 77.50 seconds.*

Applying this method to 86 GP-B passes of phase A (selected to contain at least 5 peaks), the resulting spin period values coincide well with spin data as measured by GP-B (Fig. 7a); the accuracy of the resulting inertial spin period is improved now, with an RMS value of 0.98 seconds (Fig 7b).

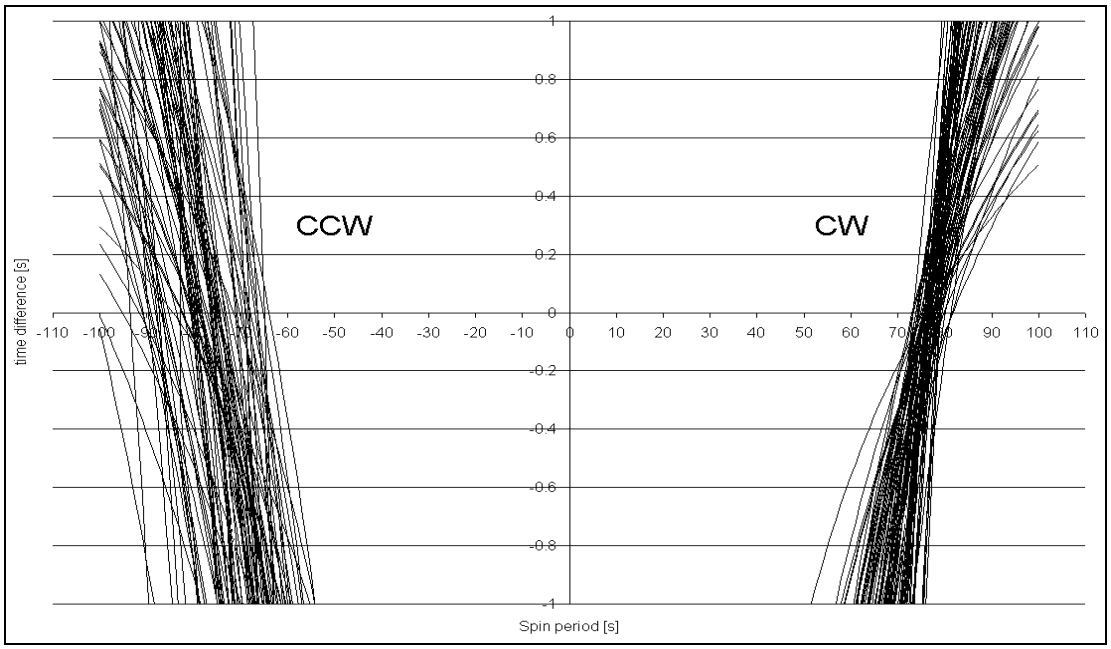

***Fig. 6:** Differences between T_{meas} and T_{sim} for 100 passes of phase A; CCW (left) and CW (right) spin directions have been simulated.*

Determination of Spin Direction

We define clockwise (CW) and counter clockwise (CCW) spin direction here as the spin of the spacecraft when looking on the LRR in pointing direction of GP-B. This spin direction of GP-B is a priori not known to us. To determine it using the kHz SLR

data, both spin directions were simulated (Fig. 6).

The results in Fig. 6 indicate that GP-B spins CW, because the spread of the result here is much less than for the CCW simulation.

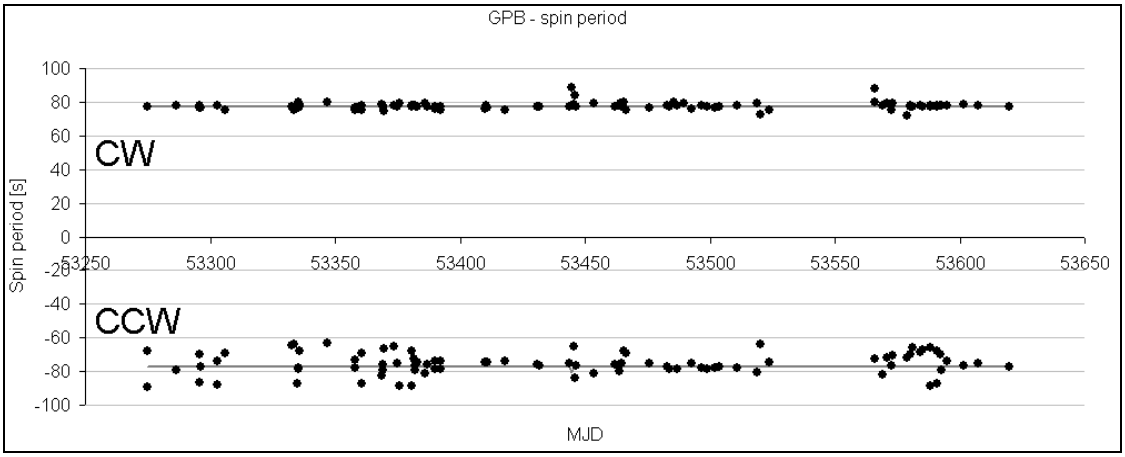

Fig. 7a: *GP-B spin period for 86 passes during phase A; positive values are for CW spin, negative for CCW spin assumed; solid lines at ±77.5 seconds indicate results of on-board spin measurements.*

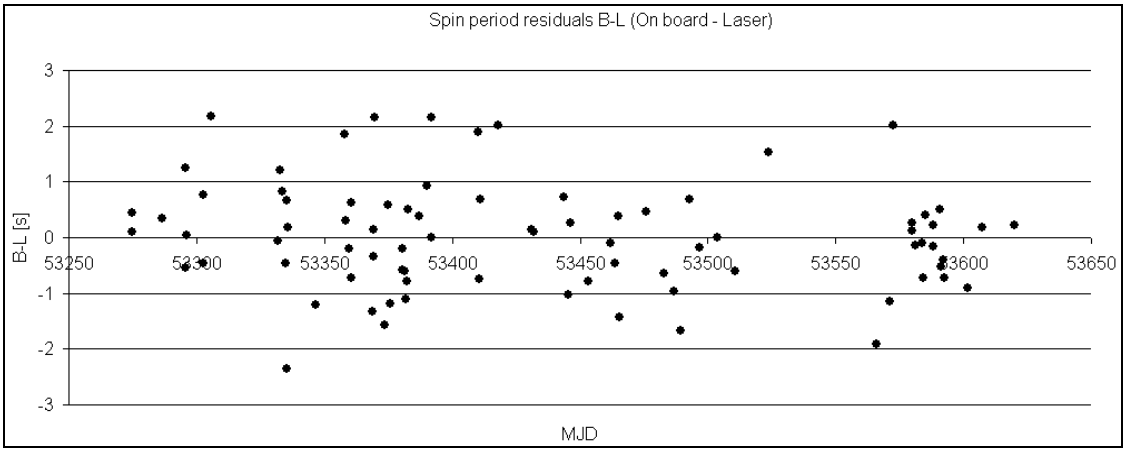

Fig. 7b: *Spin period for 86 passes of phase A with at least 5 peaks: differences to on-board spin period measurements; RMS of differences is 0.98 seconds.*

Determination of Spin Axis

Due to their periodically varying distances as seen by the SLR measurements, the eight laser reflectors generate specific patterns within the return data set, with a "modulation depth" depending on the incident angle between laser beam and GP-B's axis (Fig. 8).

This change of the modulation depth within the pass can be used to evaluate the incident angle (Fig. 8, bottom) and thus at least one orientation angle of the satellite. However, this method proved to be more inaccurate than expected, mainly due to the limited resolution of the modulation depth determination; the instrumental jitter of about 3 mm RMS of the Graz kHz SLR system for GP-B is not really adequate to determine the modulation depth variations of 0 to 6 mm with sufficient accuracy.

Looking for a more suitable method to determine spin axis, the comparison between simulations and measurements once more proved to be appropriate. For this purpose, the returns from the 9th or central retro reflector, which are vaguely visible in a few

passes, were used additionally (Fig. 9). Fitting a parabola to these returns, and determining the minimum value of the oscillations of the other 8 retro reflectors (Fig. 10), allows to fix the minimum distance between the upper and the lower curve (D), and the corresponding epoch time.

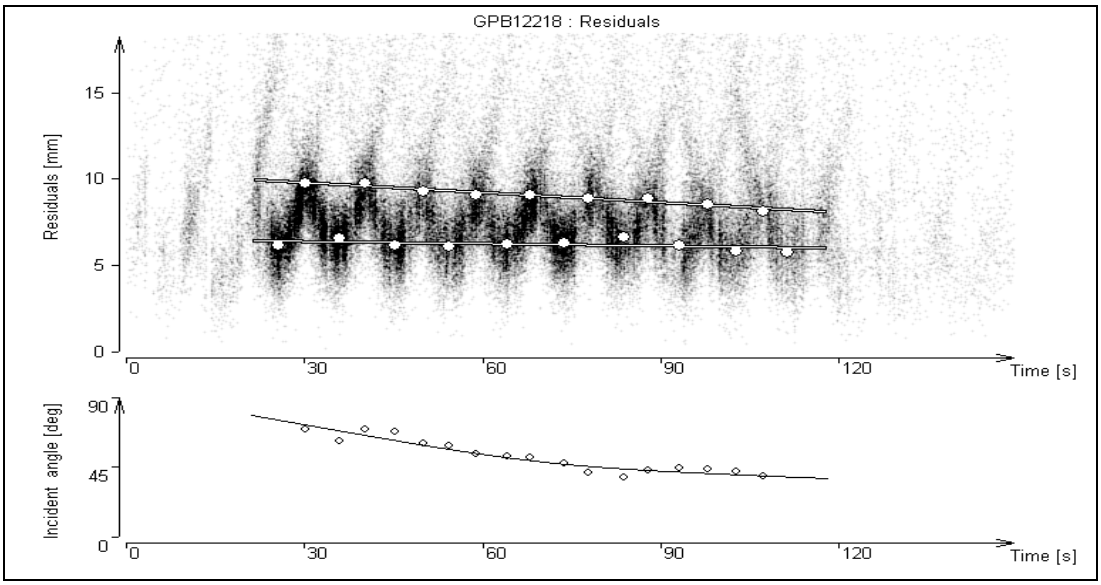

Fig. 8: *GP-B pass of DOY 122 / 2005: "Modulation depth" decreases during the pass (top); applying the known geometry of the retro reflectors, the incident angle of the laser beam can be determined (bottom).*

Running now simulations for this pass, spin axis longitude and colatitude (i.e. spin axis direction) were varied in steps of 1° each; for each spin axis direction, the spin period was calculated with the same method as described above. The goal was to find a combination spin period and spin axis direction, so that epoch time differences (between 9th retro parabola minimums of measurement and simulation) and range differences D (between simulations and measurements) are zero or close to zero.

Fig. 11 plots these differences between simulations and measurements; on the X-axis the differences in epoch time, on the Y-axis the differences in the distances D are shown; each line (set of points) represents solutions for different spin axis longitudes, and each point on these lines represents a solution for different spin axis colatitudes. The lowest line indicates a longitude of 320°, step size is 1°; zero for epoch and range differences means that the correct spin axis angles have been used in the simulation, as well as the correct inertial spin period; using this rough graph, the approximate longitude solution is between 340° and 341°, and the approximate colatitude between 73° and 74° (Fig. 11, left).

Using these values as boundaries for a more detailed simulation run with step sizes of 0.1°, we get about 341.4° for longitude, and 73.3° for colatitude, at an inertial spin rate of 77.42 seconds (Fig.11, right).

Two more GP-B passes were analyzed in this way, and the spin axis parameters determined; all results were coinciding with the on-board values with good accuracy (Table 1): standard deviation of the differences is 1.6° for colatitude, 1.77° for longitude, and 0.6 seconds for spin period.

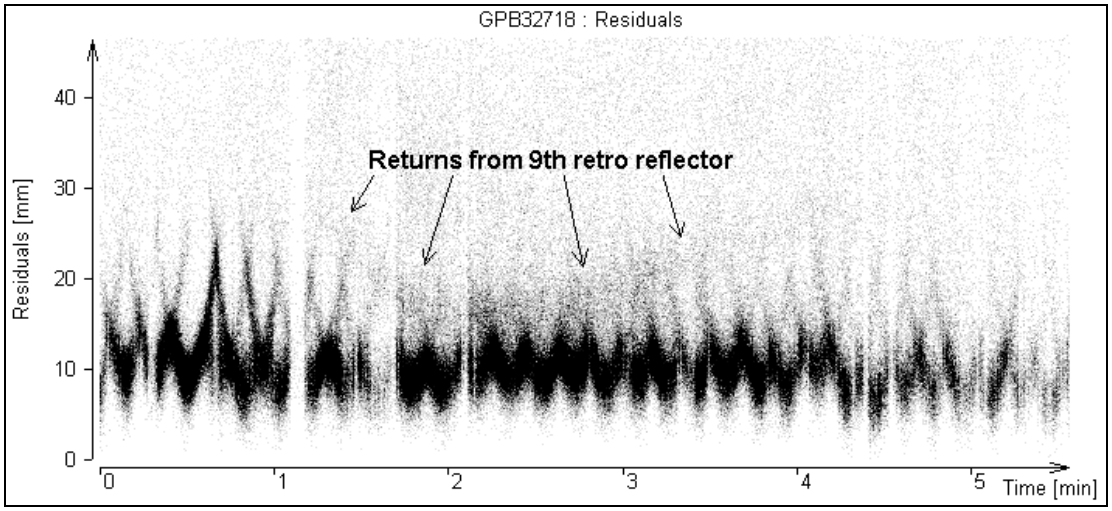

***Fig. 9:**. GP-B pass of DOY 327/2005: Vaguely visible returns from 9th retro.*

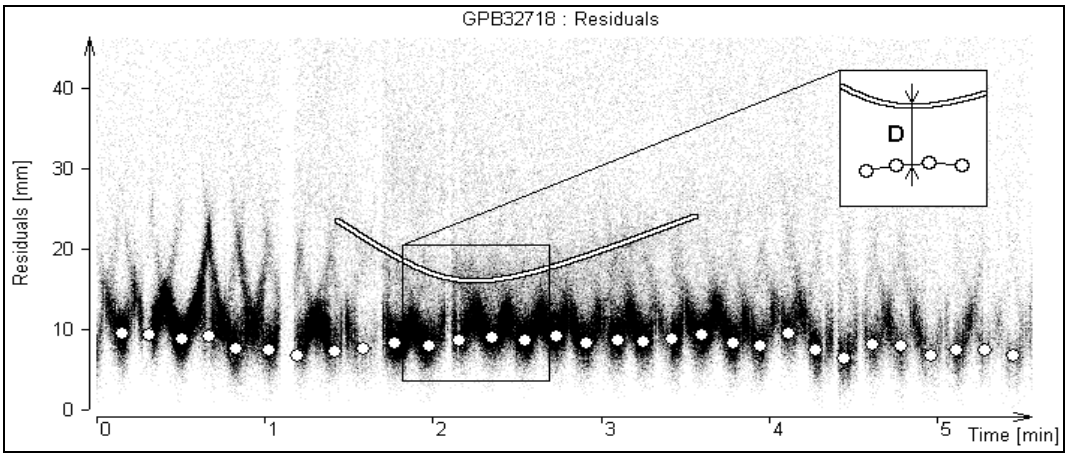

***Fig. 10:**.Parabola fitted to 9th retro returns, gives epoch time and value of "D"*

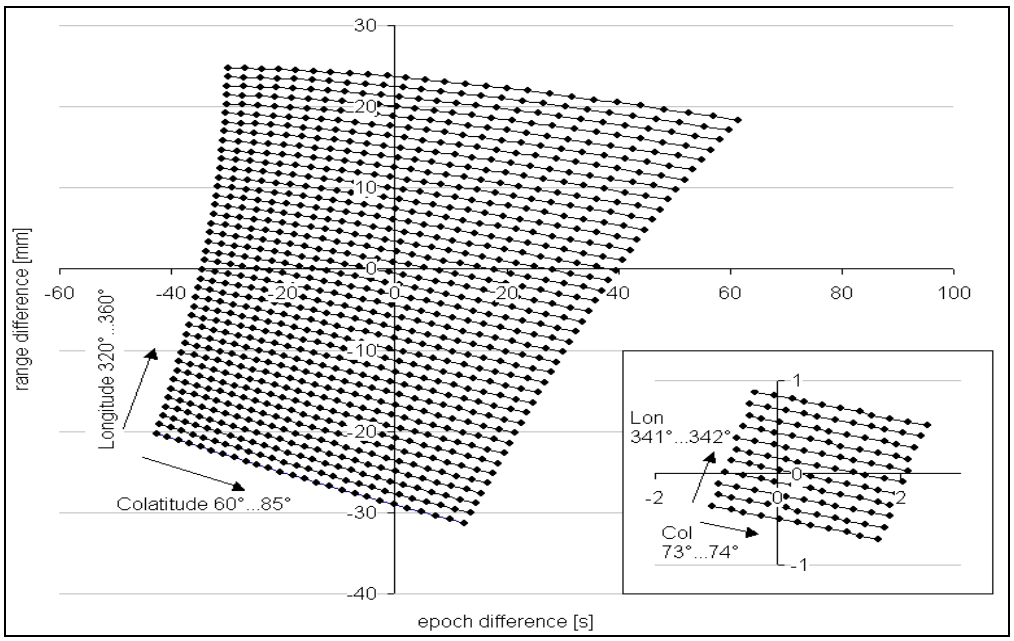

***Fig. 11:**.Simulations for Longitude and Latitude vales of GP-B Spin Axis, varied in 1°-steps (left); same with 0.1° steps around ZERO (right)*

Table 1: *Comparison of complete spin parameters for 3 GP-B passes.*

Pass date	Colatitude [deg]		Longitude [deg]		Spin period [s]	
	Calculated	IM-Pegasus	Calculated	IM-Pegasus	Calculated	On board measurements
2004-11-22 18:06	73.3	73.16	341.4	343.26	77.42	77.48
2005-04-04 9:23	71.7	73.16	339.9	343.26	76.30	77.53
2005-07-29 1:48	74.9	73.16	341.2	343.26	77.05	77.48

Conclusions and Future Aspects

Using only kHz SLR data to derive spin parameters of satellites, opens completely new possibilities and areas for present and especially for future missions; larger separations between the individual elements of the retro reflector arrays automatically would increase the resulting accuracy. Suitable LRR geometries - to allow the identification of returns from single retro reflectors - enables complete spin axis determination from kHz SLR measurements. To get a more uniform distribution of returns from retro reflectors at different locations on the satellite, it would be easy to attenuate all echoes to the single photon level, resulting e.g. in the GP-B case in a much clearer identification of the 9^{th} retro returns (Fig. 9, 10).

As more such kHz SLR stations will be operational in the very near future (Herstmonceux in the UK, SLR 2000 in USA), the availability of kHz SLR data sets will increase, allowing even more accurate spin parameters determination. As the satellite's payload for SLR is only a passive retro array, without any need for power supply or transmission bandwidth – and without major concerns about operational life time - , it might be a good main or backup device to obtain independently spin parameters of satellites, in addition to its main task of precise orbit determination via SLR.

Acknowledgment

The authors would like to thank Paul Shestople of Stanford University for providing the on-board GP-B spin rate data.

References

[1] GP-B Home Page: http://einstein.stanford.edu/

[2] LRR Manufacturer Home Page: http://www.iteinc.net/

[3] T. Otsubo, J. Amagai, H. Kunimori, and M. Elphick, "Spin motion of the AJISAI satellite derived from spectral analysis of laser ranging data", IEEE Transactions on Geoscience and Remote Sensing, Vol. 38, No. 3, May 2000.

[4] G. Kirchner, W. Hausleitner, E. Cristea, "AJISAI Spin Parameters Determination using Graz kHz Satellite Laser Ranging Data", IEEE Transactions on Geoscience and Remote Sensing, Vol. 45, No. 1, January 2007.

LAGEOS-1 spin determination, using comparisons between Graz kHz SLR data and simulations

D. Kucharski[1], G. Kirchner[2]

1. Space Research Centre, Polish Academy of Sciences, Borowiec, ul. Drapalka 4, 62-035 Kornik, Poland.

2. Space Research Institute, Austrian Academy of Sciences, Lustbuehelstrasse 46, A-8042 Graz, Austria.

Contact: kucharski@cbk.poznan.pl / Tel. +48 61 817 01 87;
Georg.Kirchner@oeaw.ac.at / Tel. +43 316 873 4651

Abstract

kHz SLR data contains unique information about the measured targets; this information allows e.g. determination of spin parameters (spin period, spin direction, spin axis orientation) of various satellites, using various methods for different spin periods / satellites: Spectral analysis for spin periods of 2 s (AJISAI (Kirchner et al, 2007)), simulations for spin periods of 77.5 s (GP-B), and comparing simulation results with kHz data for very long spin periods like LAGEOS-1 (about 5000 s).

For the long LAGEOS-1 spin periods, we developed a method to calculate spin axis orientation and spin period from Graz kHz SLR data. This method is based on simulation of returns from each retro reflector, with spin period and spin axis orientation as input parameters. Varying these parameters, the simulation generates retro tracks similar to those seen in the kHz SLR data; comparing simulated and measured tracks, allows determination of spin period, and spin axis orientation. Applying this method to a set of LAGEOS-1 passes - covering a period of 178 days – shows also the slow change of the LAGEOS-1 spin axis direction with time.

***Keywords**: satellite laser ranging, LAGEOS-1, satellite spin*

Introduction

LAGEOS-1 and LAGEOS-2 are identical satellites in circular orbits, about 5,900 km above Earth's surface. Both satellites are spheres with 60 cm diameter, covered with 426 cube corner reflectors (CCRs) arranged in 20 rings symmetrically with respect to the satellite equator (Fitzmaurice et al., 1977) . Because the satellites are totally passive, their orbital motions are affected only by the natural perturbations. In this paper, we analyse only kHz SLR data of LAGEOS-1, due to its very low spin rate.

Perturbations can be of gravitational, non-gravitational (for example: Yarkovsky effect, Yarkovsky-Schach effect) or magnetic nature. SLR distance measurements to the satellites allow precise determination of these orbital perturbations and consequently identification of their origin. The more accurately we can determine the effect of perturbations, the more reliably we can obtain the geodynamical parameters of the Earth, and the relativistic effects in the near space (Ciufolini and Pavlis, 2004). It is expected that a detailed knowledge of LAGEOS-1 spin behaviour should improve the accuracy of such analysis, and will help to identify and confirm the source and magnitude of the (unknown) perturbations, which are introduced presently as empirical accelerations in actual models.

Up to now two methods were used to calculate spin parameters of LAGEOS satellites: frequency analysis of full rate SLR data (Bianco et al, 2001) and analysis of

photometric observations. The frequency analysis works well if the spin rate is not too low (e.g. 23.5 s for LAGEOS-2 in May 2000 gives good results in Bianco et al, (2001), but is not applicable anymore for larger spin periods, like the expected 5000 s for LAGEOS-1 in 2004 (Andres et al., 2004). Photometric measurements of LAGEOS-1 spin parameters were performed until 1997, when they were ceased because of a too low spin rate. In total, 57 photometric observations were carried out for this satellite (Andres et al., 2004), which allowed verification and improvement of the models of its spin motion. The most accurate model describing changes in the parameters of LAGEOS-1 spin is LOSSAM (Andres et al., 2004). According to this model, LAGEOS-1 started the third phase of its life in 1999, where the influences on spin parameters by magnetic, gravitational and non-gravitational torques are of the same order of magnitude. Bertotti and Iess (1991) have predicted that at this phase LAGEOS-1, having reached an extremely low spin rate, will start tumbling more and more, rapidly changing orientation of the spin axis, with chaotic dynamics.

SLR Graz kHz laser measurements

Usually, SLR stations measure distances to satellites with laser repetition rates of 5 or 10 Hz. The Graz SLR station was the first station to measure with a laser repetition rate of 2 kHz (Kirchner and Koidl, 2004). Because of the very short 10 ps laser pulses, and the single photon detection system, the measurements are not only very precise (2–3 mm single shot RMS), but also allow identification of retro – reflector tracks in the data, easily seen due to their slightly different distances.

After a successfully measured satellite pass, the differences between measured and predicted distances are calculated. From these residuals the systematic trends are eliminated, e.g. by using polynomials; plotting these residuals (Fig. 1), different tracks from various retro-reflectors (or groups of them) can be identified easily. Residuals of nearer satellite prisms are on the bottom (satellite front), and residuals originating from more distant prisms are more towards the top in this figure.

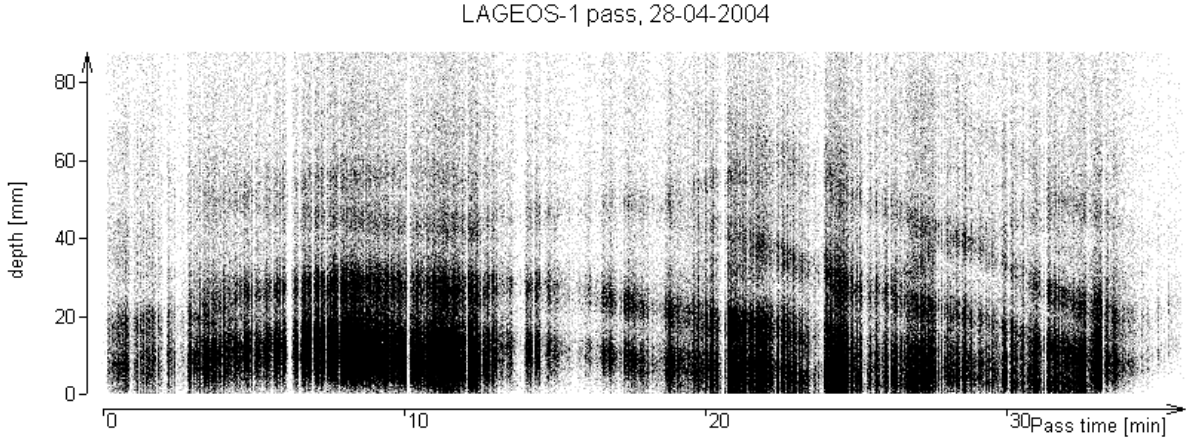

Fig. 1. *Range residuals of a LAGEOS-1 pass, measured by Graz kHz SLR system, 28-04-2004, 2 a.m. (P1)*

The residuals plotted in Fig. 1 refer to a LAGEOS-1 pass of April 28th, 2004 (P1). During the 35 minutes of the pass, more than 500,000 returns were measured. The majority of the returns come from the nearest retro-reflectors; the detection probability for returns from more distant retro – reflectors on the satellite's sphere is decreasing. The reason for this effect is the geometry between the incident laser beam and the CCR. Total internal reflection of LAGEOS-1 optical retro - reflectors depends

on the angle between the incident laser beam and optical axis of the CCR as well as on the azimuth angle giving the direction of the incident beam about the normal to the front face of the CCR (Arnold, 1979; Otsubo and Appleby, 2003).

Identification of the single prism tracks – the method

The tracks in Fig. 1 are due to the passage of retro – reflectors through the field of view of the telescope; thus they contain information on the satellite spin (Arnold et al., 2004). To recognize spin parameters out of the geometry of these spin tracks we developed a new method based on simulations of SLR measurements. The model used in these simulations is divided into two parts. The first part (macro-model) contains the Earth's rotation, the site position in ITRF2000 (Altamimi et al., 2002) and the orbital motion of the satellite. The second part (micro-model) contains the retroreflector-array arrangement and the range correction function (Fitzmaurice et al., 1977). In present study the model does not contain CCR transfer function (Arnold, 1979). The range correction function describes the photon's time of flight delay when the photon is going through the glass of the CCR. This correction depends on refractive index of the glass and the angle of incidence.

The geometry of range residuals distribution depends on spin parameters of the satellite: spin axis orientation and spin period. To calculate spin parameters it is necessary to determine epochs of the spin tracks and their tilt angles. The pass shown on Fig. 1 contains horizontal and tilted CCR tracks.

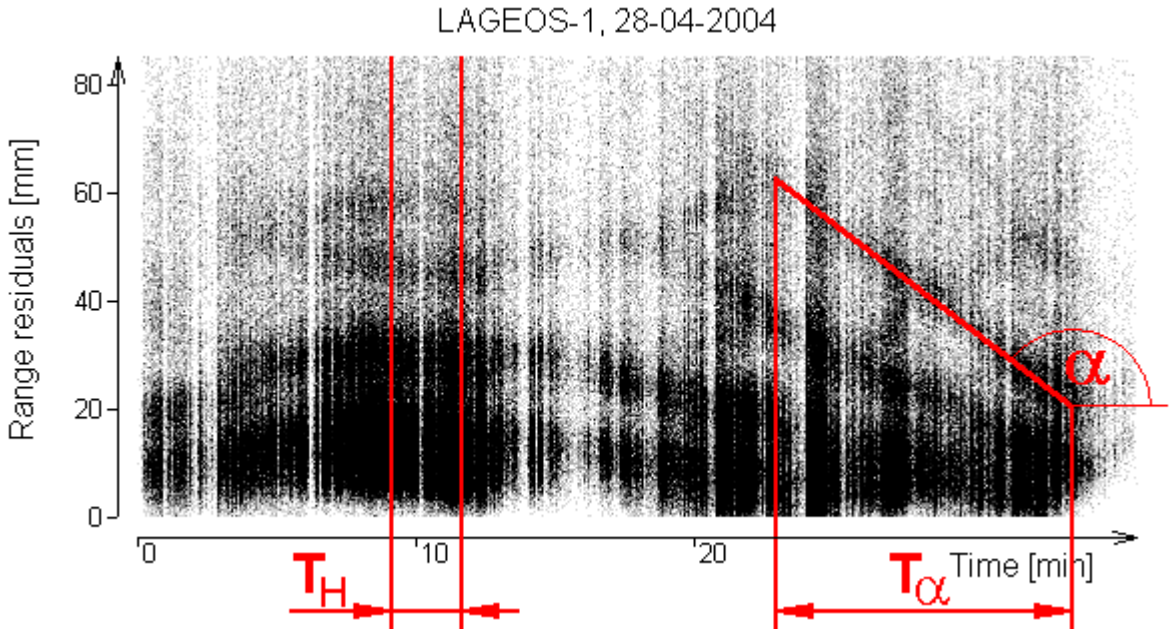

Fig. 2. *Range residuals distribution: T_H - epoch range of horizontal tracks, T_α - epoch range of α-tilted track, pass start 28-04-2004, 2 a.m.*

By using simulations it is possible to generate range residuals for every CCR distributed over the visible satellite's surface. Figure 3 presents examples of simulated CCR's trajectories for different spin parameters of the pass presented on Fig 2. For both charts spin period remains the same, but the second case was generated for different spin axis orientation: both angles (longitude and co-latitude) were increased by 10°. The geometry of the CCRs trajectories is very sensitive for spin parameters.

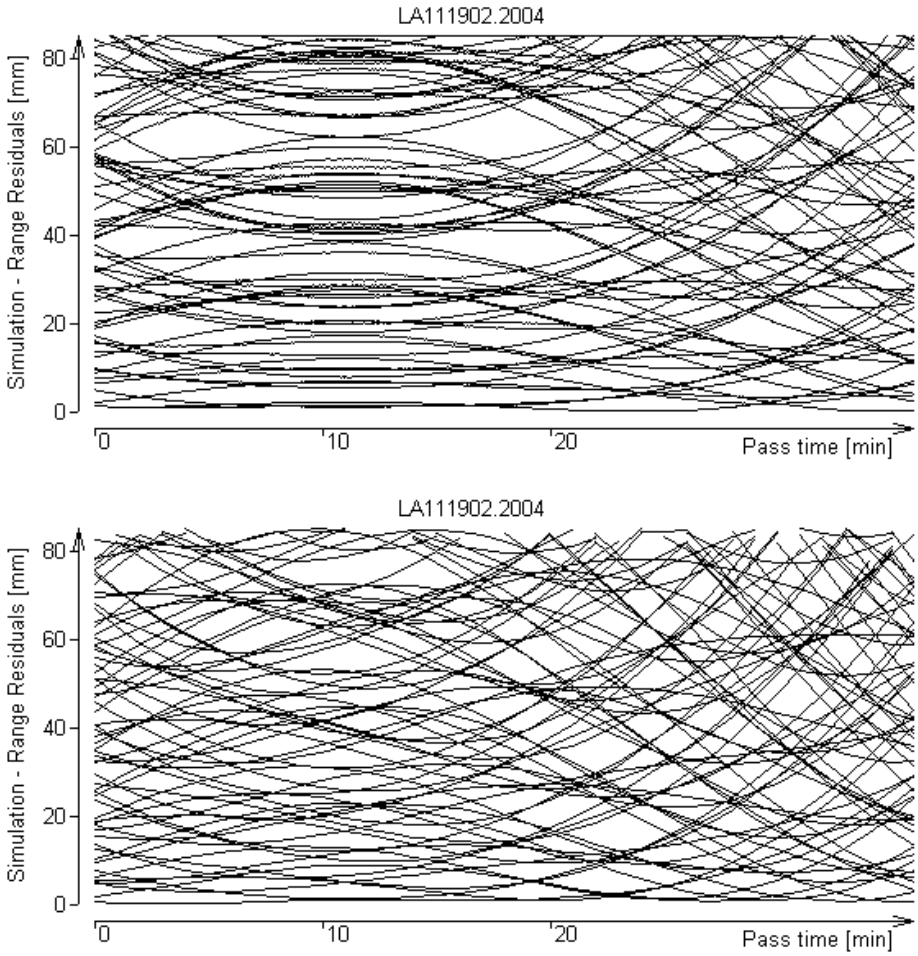

Fig. 3. *Simulations of the CCR's trajectories for the pass presented on fig 1, for both cases spin period stays constant, but spin axis orientation for the bottom situation is shifted by 10° in longitude and colatitude.*

Spin parameters determination

The LAGEOS-1 pass shown in Fig. 2 (P1) shows two significant kinds of range residuals distribution - horizontal and α-tilted - which allows determination of the satellite's spin rate. LOSSAM predicts a spin period of about 5,000 s for LAGEOS-1 for the first half of 2004. Therefore we simulated range residuals for the pass P1 for spin periods T_S from –8,000 s to –3,000 s and from 3,000 s to 8,000 s with 50 s steps, and for all spin axis orientations with 1° steps.

Figure 4 shows results of simulations for all possible spin axis orientations (longitude and colatitude), for a spin periods of T_S=-6,000 s and T_S=6,000 s. The top chart presents amounts (right scale – color bar) of α-tilted spin tracks in T_α epoch range for all spin axis orientations, the middle chart presents amounts of flat spin tracks in T_H (T_α and T_H are given for the pass presented on Fig. 2). During all simulations the algorithm was searching for simulated α-tilted CCR tracks within $\alpha \pm 5$ deg. The bottom charts (Fig 4) show the sum of the top and the middle charts, evaluated pixel by pixel; as can be seen, for some spin axis orientations both kinds of spin tracks can exist. Such common spin axis orientation areas are the biggest for –6,000 s (counter-clockwise rotation) and 6,000 s (clockwise rotation), therefore those spin periods were chosen for further investigation.

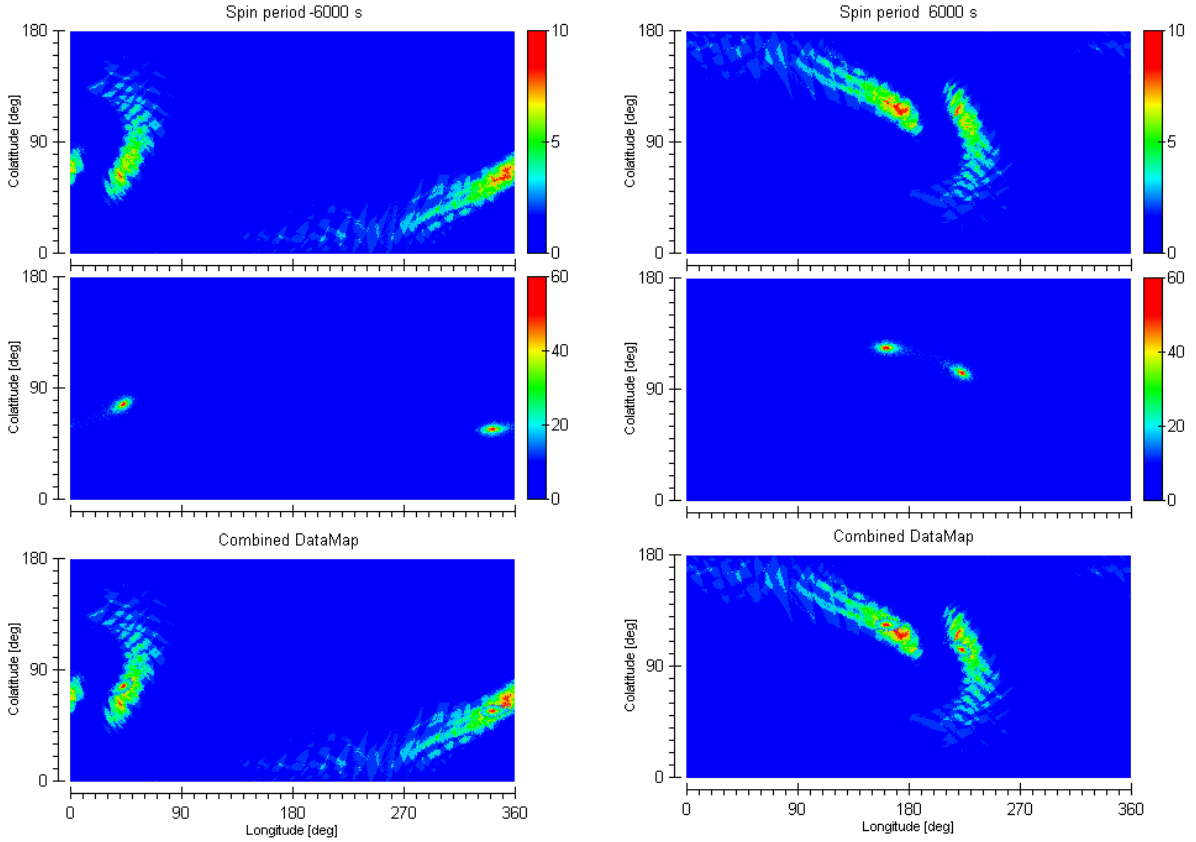

Fig. 4. *Simulation results for spin period of T_S=-6000 s (left) and T_S=6000 s (right); Top: Amounts of a-tilted spin tracks; Middle: Amounts of horizontal spin tracks; Bottom: Sum of Top and Middle, pixel-by-pixel*

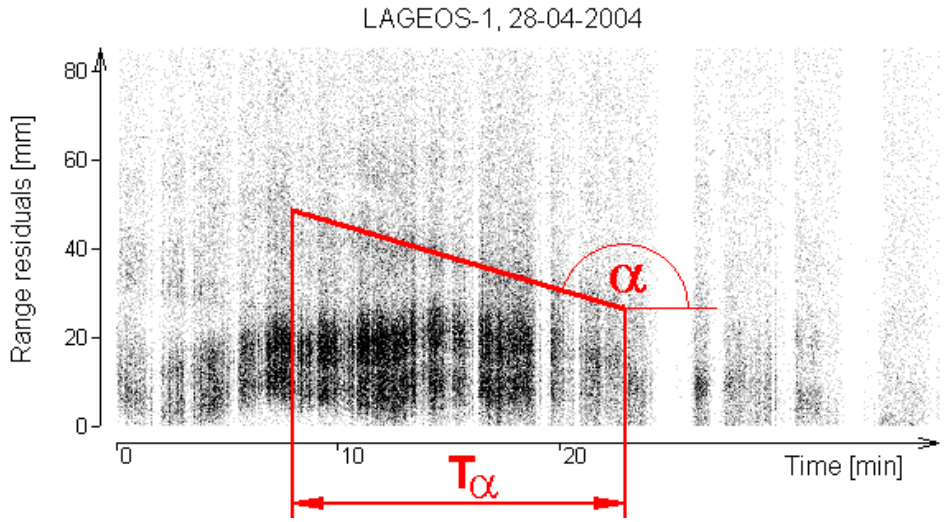

Fig. 5. *Range residuals of LAGEOS-1 pass tracked 12 hours later (P2), pass start 28-04-2004, 2 p.m.*

For both spin periods it is possible to detect two different solution areas (Fig. 4, the bottom charts), due to the symmetrical arrangement of the CCRs over the surface of the satellite. After processing four solutions were obtained, two for CW and two for CCW spinning. To identify which is the real one we used a LAGEOS-1 pass (P2) tracked 12 hours after the main pass (P1) – Fig. 5.

Supposing that spin parameters of the satellite will not change significantly during 12 hours (from pass P1 to pass P2), one of the solutions determined for P1 should be the solution also for pass P2. Figure 6 presents three charts; the top one shows spin axis orientation solution for P1 and the middle chart for P2. The bottom chart shows common area of solutions for these two passes (pixel by pixel comparison); the appropriate spin axis orientation for both P1 and P2 was calculated as a mean value of this area.

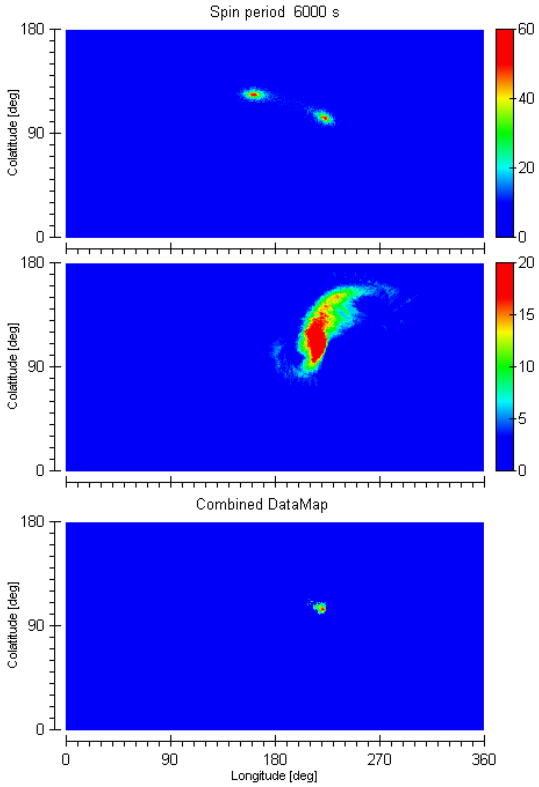

Fig. 6. *Simulation - results; Top and middle: solutions for passes P1 and P2; Bottom: common area of the solutions*

Using this pass-to-pass method reduces the amount of possible solutions from four to one; the spin parameters of LAGEOS-1 calculated from these two passes are: spin period (CW) T_S=6,000 s, spin axis orientation: colatitude=103.8 deg, RMS=3.66 deg, longitude=224.2 deg, RMS=3.76 deg. All parameters are expressed in the J2000 inertial reference frame.

This pass-to-pass method was used to process 33 passes during 178 days of year 2004. Figures 7 and 8 present results for colatitude and longitude of spin axis orientation. The results were obtained for spin period T_S=6,000 s, mean value of RMS for all colatitude results is RMS_{COL_mean}=5.87 deg, and for longitude RMS_{LON_mean}=7.19 deg.

For both angles the scatter around the fitted trend function is visible and has similar magnitude. That may be caused by inaccuracy of the used method or even by chaotic changes of the spin axis precession. The trend function of colatitude values shows sinusoidal decreasing during the investigated time period, while the longitude angle is more stable.

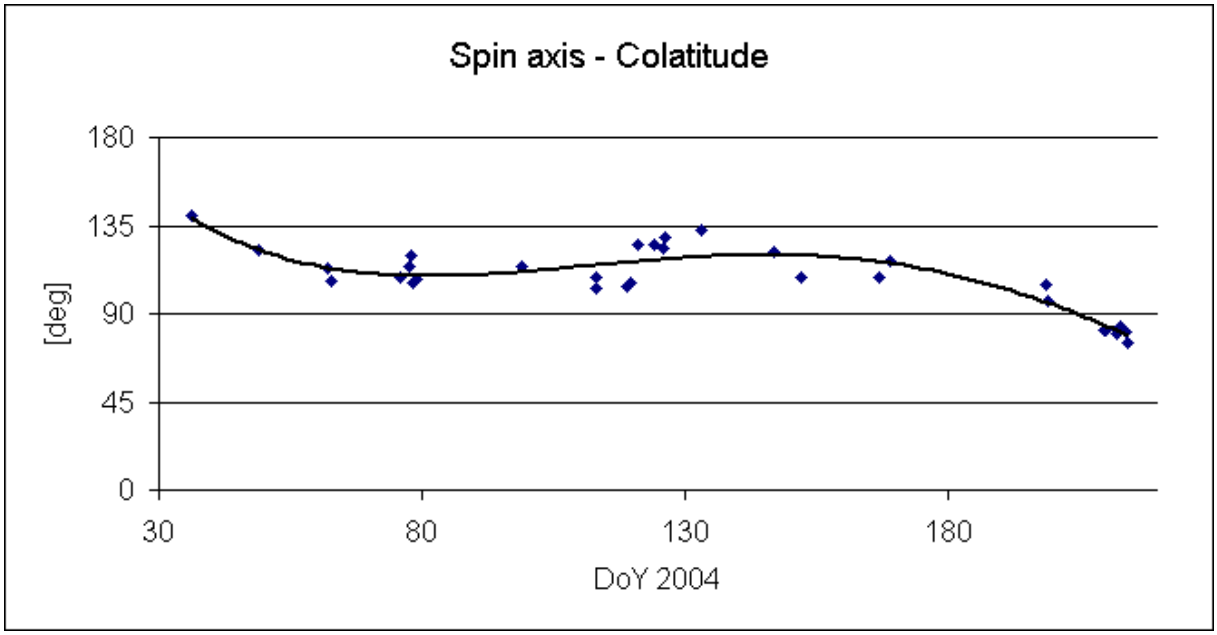

Fig. 7. *Time-series of colatitude angle observations of the spin axis of LAGEOS-1, and trend function*

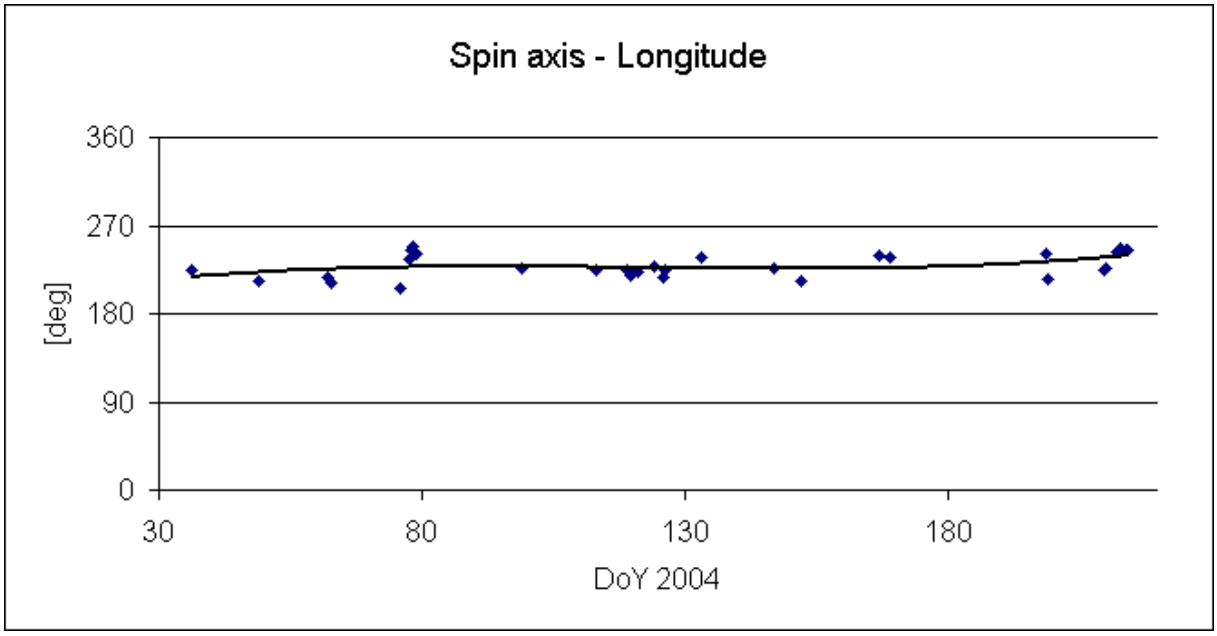

Fig. 8. *Time series of longitude angle observations of the spin axis of LAGEOS-1, and trend function*

Conclusions

The analysis presented in this paper identifies spin tracks in kHz SLR measurements to LAGEOS-1, and uses them to fully determine the spin parameters of this very slowly spinning satellite. This was possible by identifying the geometry of the observed tracks and looking for similar geometries in simulations generated for various spin parameters. This process allows to find several possible solutions, but with the pass-to-pass method it is possible to find a single common solution for two consecutive passes. This method can be applied only when spin parameters do not change significantly between the two analysed passes. Only one out of 33 investigated

passes contains both horizontally and α-tilted CCR tracks, which are both necessary to determine the spin period of the satellite. The simulation model used for presented investigation is missing CCR energy transfer function, thus obtained results contain additional error. The transfer function will be taken into account with next version of the model and then analysis process will be repeated.

The accuracy of our method is a few times worse than that of photometric measurements. However, for long spin periods kHz SLR measurements and this simulation-based method is the only source of information about spin parameters of LAGEOS-1.

kHz SLR measurements, as started for the first time at the Graz SLR station, have opened new possibilities, allowing determination of the satellite spin parameters when all other methods fail. Additionally, the expected increase of the number of kHz SLR stations in the near future will improve the accuracy of spin parameter determination by a few orders of magnitude.

Acknowledgments

This work has been supported by the Ministry of Science and Information of Poland under grant No. 4T12E 062 29.

References

[1] Altamimi, Z., Sillard, P., Boucher, C. ITRF2000, A new release of the International Terrestrial Reference Frame for Earth science applications, J. Geophys. Res. 107(B10), 2214, 2002

[2] Andrés, J. I., Noomen, R., Bianco, G. et al., Spin axis behavior of the LAGEOS satellites, J. Geophys. Res., 109(B6), B06403, doi:10.1029/2003JB002692, 2004

[3] Arnold, D., Method of calculating retroreflector-array transfer functions, Spec. Rep. 382, Smithon. Astrophys. Obs., Cambridge, Mass.,1979

[4] Arnold, D., Kirchner, G., Koidl, F., Identifying single retro tracks with a 2 kHz SLR system – simulations and actual results, 14th ILRS Workshop, 2004

[5] Bertotti, B., and L. Iess, The rotation of LAGEOS, J. Geophys. Res., 96(B2), 2431–2440, 1991

[6] Bianco, G., Chersich, M., Devoti, R. et al., Measurement of LAGEOS-2 rotation by satellite laser ranging observations, Geophys. Res. Lett., 28(10), 2113–2116, 2001

[7] Ciufolini, I., Pavlis, E., A confirmation of the general relativistic prediction of the LenseThirring effect, Nature, 431, 958-960, 2004

[8] Fitzmaurice, M.W., Minott, P.O., Abshire, J.B. et al., Prelaunching testing of the Laser Geodynamic Satellite (LAGEOS), NASA Technical Paper 1062, NASA, 1977

[9] Kirchner G., Hausleitner W., Cristea E., "Ajisai Spin Parameter Determination Using Graz Kilohertz Satellite Laser Ranging Data", IEEE Trans. Geosci. Remote Sens., vol. 45, no. 1, pp. 201-205, Jan. 2007

[10] Kirchner, G., Koidl, F., Graz KHz SLR System: Design, Experiences and Results, 14th ILRS Workshop, 2004

[11] Otsubo, T., Appleby, G., System dependent center-of-mass correction for spherical geodetic satellites, J. Geophys. Res., 108(B4), 2201, doi:10.1029/2002JB00209, 2003

Measuring Atmospheric Seeing with kHz SLR

Georg Kirchner[1], Daniel Kucharski[2], Franz Koidl[1], Jörg Weingrill[1]

1. Austrian Academy of Sciences, Institute for Space Research, Graz
2. Space Research Centre, Polish Academy of Sciences, Borowiec, Poland

Contact: Georg.Kirchner@oeaw.ac.at ; kucharski@cbk.poznan.pl ; Franz.Koidl@oeaw.ac.at ; Joerg.Weingrill@oeaw.ac.at

Abstract

During night-time kHz SLR operation in Graz, we use an ISIT camera to see satellites, stars, and also the backscatter of the transmitted kHz laser beam (Fig. 1). This backscatter image of the laser beam shows a beam pointing jitter in the order of several arcseconds, caused by the actual atmospheric conditions ("Seeing").

Using real time image processing, we determine the area of this beam pointing jitter, and derive the actual astronomical seeing values. These values depend not only – as usual for optical astronomy - on actual atmospheric conditions and on elevation of telescope, but also on the angular speed of telescope motion. In addition, the seeing values are considerably bigger (worse) during winter time, when – due to heating and poor isolation of the Graz observatory - the air above the observatory roof is significantly more turbulent than during the other seasons.

This beam pointing jitter due to atmospheric turbulence can reach a similar magnitude as the laser beam divergence; it spoils our pointing accuracy, affecting our return rate especially from higher satellites. To reduce these effects, we are planning to use a fast steering mirror, which is controlled by the ISIT image derived laser beam pointing offsets.

Introduction

The ISIT camera observes the backscatter of the transmitted laser beam; the image is transferred into the PC via a standard frame grabber. The software (written in C++) now uses the brightness of each pixel, to find out the borders of the laser beam image, and to determine the coordinates of the peak. The offset of the peak from the center (as defined by the illuminated reticle, visible in Fig. 1), is kept as a result for each processed image. This image processing at present is running with 25 Hz, and can handle each ISIT image.

The offsets of the laser beam pointing show variations in the several arcsecond range, and with frequencies between few Hz up to 25 Hz.

Possible reasons for the Laser Beam Pointing Jitter (other than atmosphere)

To verify that this jitter in laser beam pointing is NOT caused by the laser itself, we installed a Laser Beam Monitor at the exit window of the laser box (Fig. 2).

A mirror reflects a small portion of the laser beam (<< 1%) on a CCD chip; the CCD image is monitored by a PC, with up to 30 fps; for each image, the PC calculates the center coordinates (X/Y) of the laser beam, and stores single frame center coordinates and / or averaged values. This data sets (Fig. 3) show that the pointing stability of the laser at the output window of the laser box is in the order of a few microrad (<< 1", more or less within the measurement accuracy); there is no indication of a laser beam induced pointing jitter, as seen in the atmospheric backscatter images. The only visible effect is a very fast (few seconds) warm-up time at start of firing (Fig. 3)

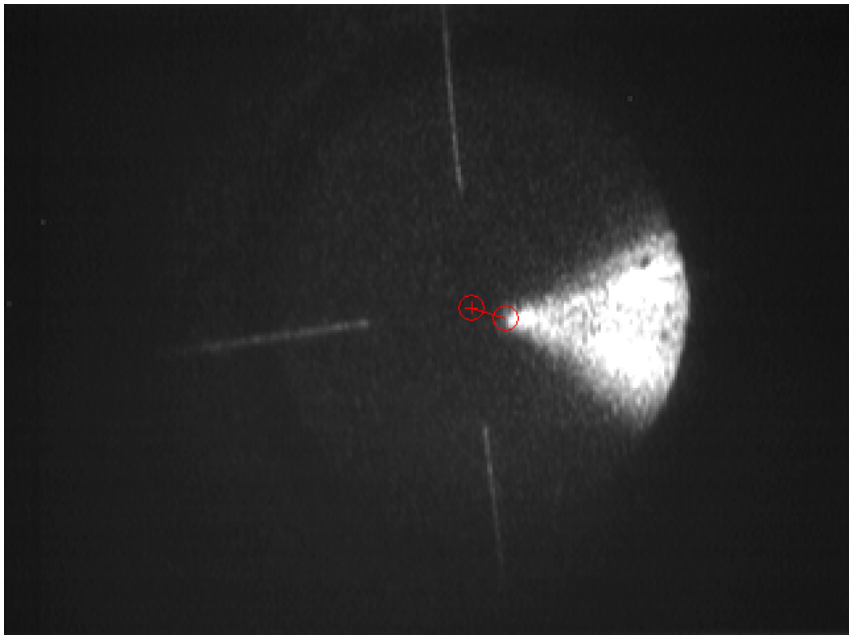

Fig. 1: *ISIT image, with laser beam backscatter, laser beam peak as determined by image processing, and its offset from the center. This offset shows a pointing jitter due to atmospheric turbulence*

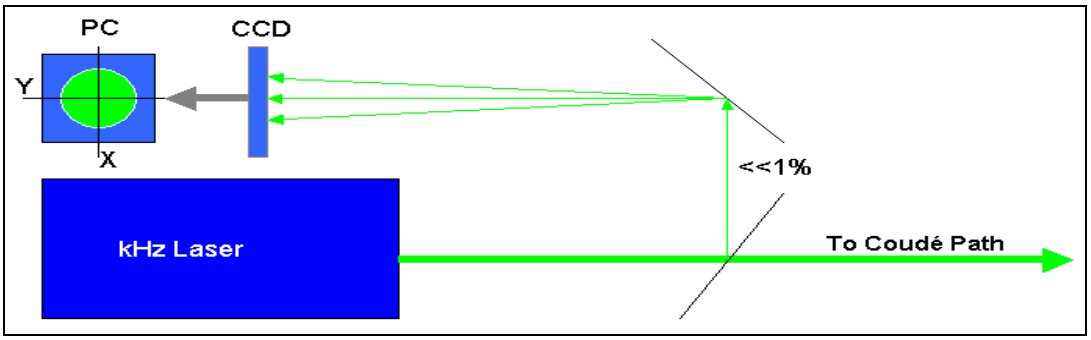

Fig. 2: *Laser Beam Monitor*

Another possibility for the observed laser beam pointing wobble is the mount itself; but tests with fixed mount showed the same wobble of the laser beam pointing.

Laser Beam Pointing Jitter: It is due to atmosphere !

We concluded that the Laser Beam Pointing Jitter is caused by atmospheric micro-turbulences (atmospheric "seeing"); after talking with astronomers working in Graz, we expected seeing values of about 2-4 arcseconds as an average, with expected frequencies from a few Hz up to a few 10 Hz.

However, our measurements usually showed higher seeing values, ranging from about 3" up to more than 8"; there are several reasons for that:

- The fast moving SLR telescope, instead of a more or less constant pointing (or only slow moving) astronomy telescopes; the atmospheric conditions during SLR tracking are therefore changing much faster;
- Heating of the – almost NON-isolated – observatory in cold winter nights; the leakage causes heating of the surrounding air, which heavily degrades seeing; and most astronomy work at the Graz observatory is done usually in autumn, with almost NO heating of the rooms;

- SLR in Graz is usually done down to 10° elevation and lower, where seeing values are increasing.

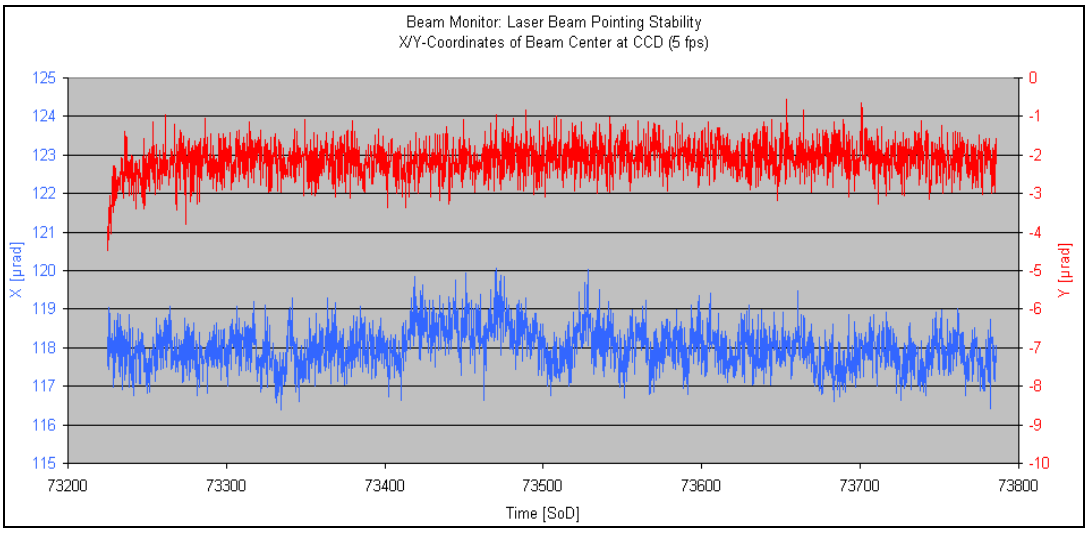

Fig. 3: *X/Y coordinates of Laser Beam Center, 10 minutes of routine SLR operation.*

What are the effects for SLR ?

The minimum laser beam divergence of SLR Graz is about 5”; with a pointing jitter caused by seeing values up to 3” to 8” (and sometimes worse) the “hit rate” or pointing accuracy will decrease (Fig. 4), reducing the return rate.

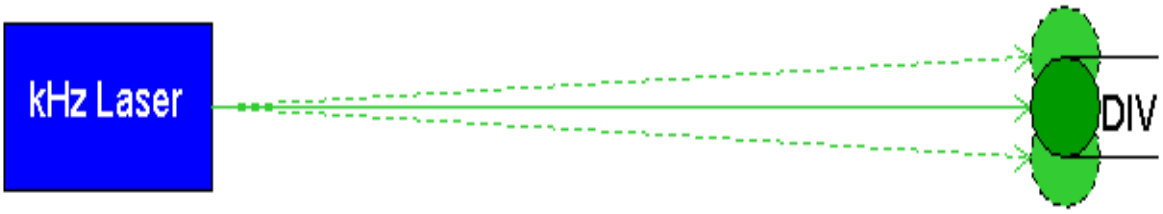

Fig. 4: *Atmospheric turbulences cause laser beam jumping*

Verifying the Seeing Values

To check and verify the seeing values, as measured by the beam pointing jitter, we used the standard DIMM (Differential Image Motion Monitor; Hartmann – Shack) method: With an additional, standard telescope we observed e.g. the polar star; a mask with 2 small holes at a specified distance is placed at the entrance pupil of the telescope (Fig. 5); a CCD (defocused; placed with some offset from the focal plane) monitors the 2 spots created from the star light and the two holes; all images are stored on the PC.

The atmospheric turbulences cause the dual star images to move relatively to each other; this relative motion is measured in the PC, and allows calculation of the atmospheric seeing values.

A typical result of such seeing measurements is shown in Fig. 6; showing an average seeing value of 3” to 4”; it was made in summer time (no heating), at 45° elevation (polar star) and with constant pointing (star).

Seeing Values Derived from kHz Laser

Using the ISIT-Camera and the image processing programs- as described at the beginning - we monitored the atmospheric seeing values automatically during routine

SLR operation for several months; due to the method, we were able to collect seeing values along each tracked pass, and to correlate it with azimuth and elevation of each pass. As an example, an AJISAI pass with about 50° maximum elevation is shown in Fig. 7; tracking started / stopped at about 10° elevation; the correlation between elevation and seeing is obvious for this pass; however, other passes showed sometimes completely different values. Such a different pass is shown in Fig. 8: an ENVISAT pass, with a maximum elevation of <30°, starts with the usual decrease of the seeing value with increasing elevation; however, it then shows a significant INCREASE.

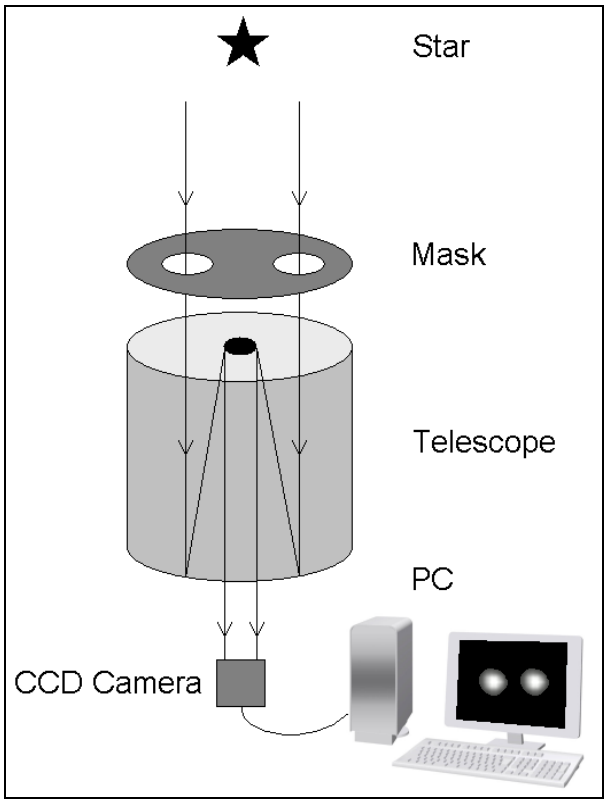

Fig. 5: *Differential Image Motion Monitor (DIMM) / Hartmann – Shack method.*

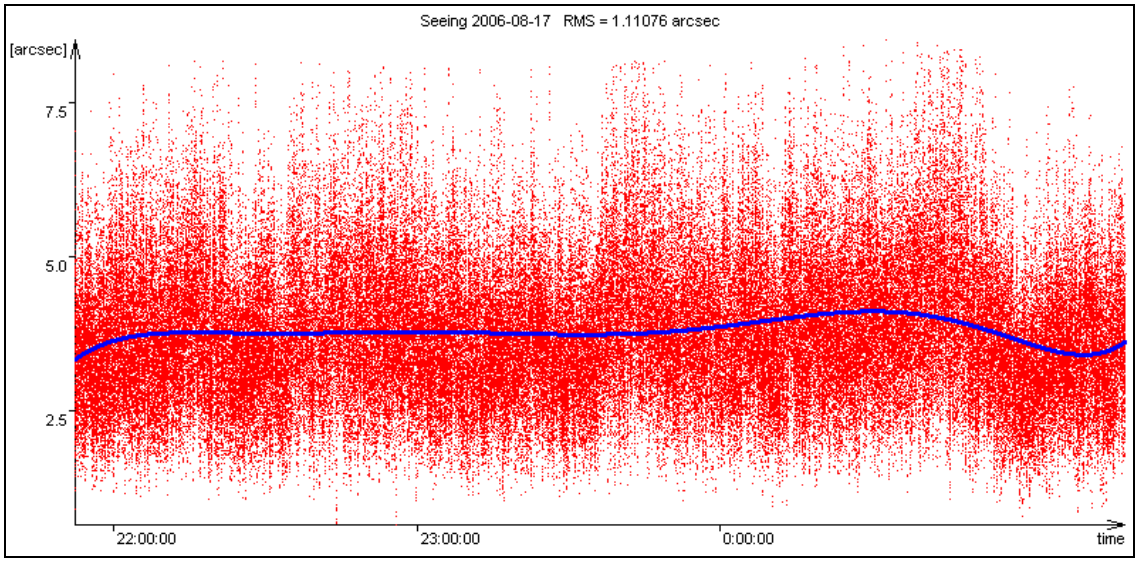

Fig. 6: *Seeing Values measured with DIMM: Summer night, polar star used.*

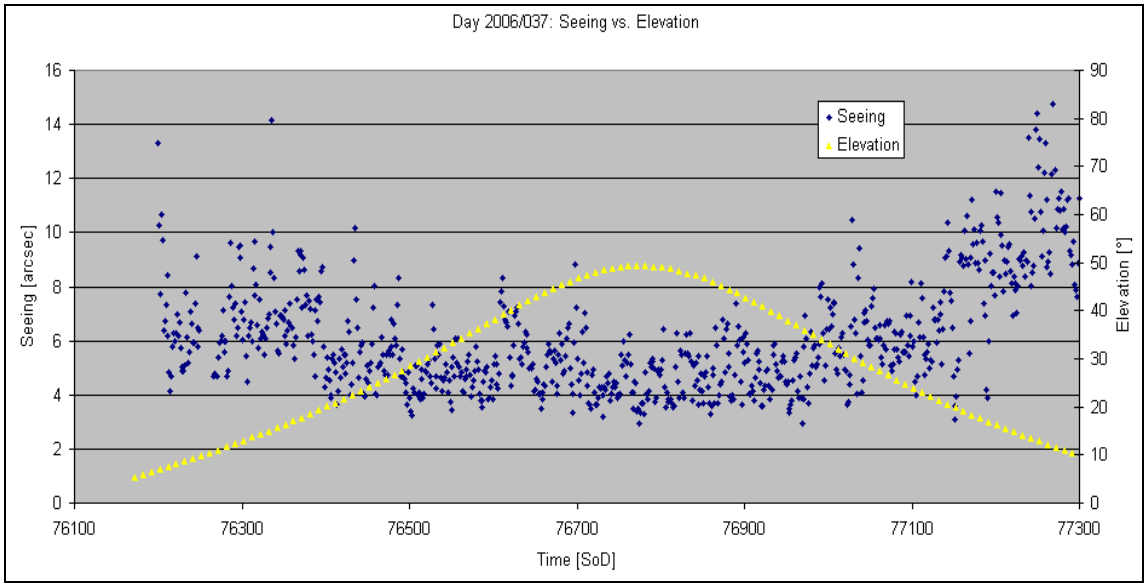

Fig. 7. *Ajisai: day of year 2006 / Day 037: Seeing changes with elevation.*

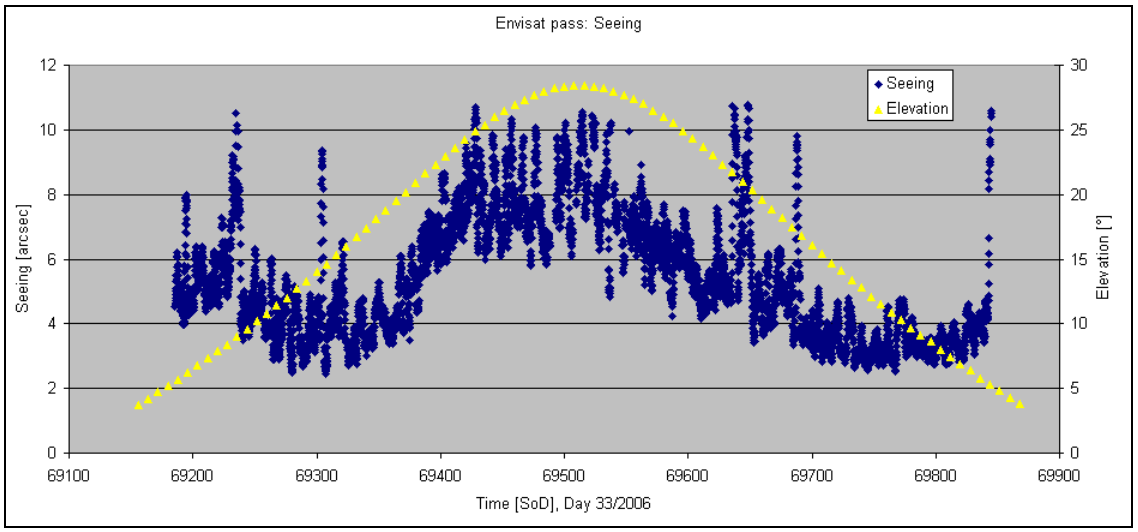

Fig. 8: *Envisat: day of year: 33, < 30° Elevation*

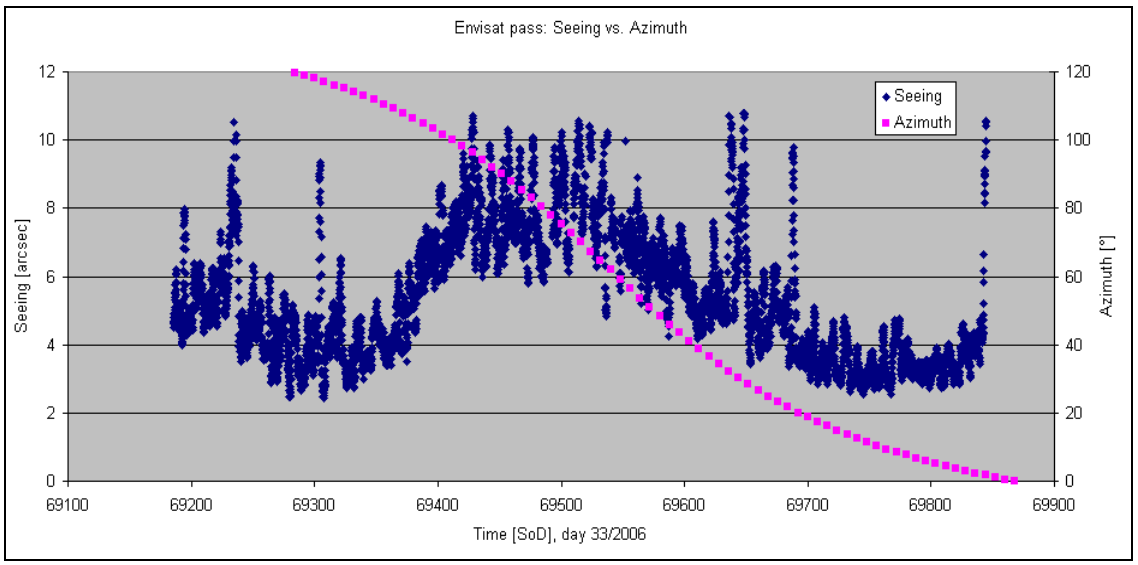

Fig. 9: *At 90° Azimuth: => Obs. Roof, Heating Influence*

The explanation for such a strange behaviour: At this time we started to track (at 90° azimuth) along / above the observatory, where the leakage of the heated building caused increasing turbulence, and hence increasing seeing values (Fig. 9).

Future plans:

We will continue to monitor atmospheric seeing values along the laser beam path during routine SLR operation at night; at least we should get some valuable statistics about the seeing values at the observatory (no such records exist here up to now). In addition, there are plans to install a Fast Steering Mirror (FSM) at the laser bench, to be able to compensate at least partially the beam pointing jitter, using the actual pointing offsets of the laser beam as derived from the ISIT images as control input to the FSM. The goal is to increase return rate from high satellites, like GPS, Giove etc.